JOURNAL OF CATALYSIS 127, 393–420 (1991)

Expanded Lattice Ruthenium Pyrochlore Oxide Catalysts

I. Liquid-Phase Oxidations of Vicinal Diols, Primary Alcohols, and Related Substrates with Molecular Oxygen

TIMOTHY R. FELTHOUSE,[1] PHILIP B. FRAUNDORF,[2] ROBERT MARK FRIEDMAN, AND CLAIRE L. SCHOSSER[3]

Central Research Laboratories, Monsanto Company, St. Louis, Missouri 63167

Received April 3, 1990; revised July 27, 1990

Ternary ruthenium oxide oxidation catalysts are reported that function directly with molecular oxygen for the conversion of oxygenated hydrocarbon substrates to carboxyl-containing products. The oxide catalysts have an expanded lattice pyrochlore structure with the general composition $A_{2+x}Ru_{2-x}O_{7-y}$ (A = Pb, Bi; $0 < x < 1$; $0 < y \leq 0.5$). These pyrochlore oxide catalysts possess high surface areas, may be used either as powders for batch autoclave reactors or granules for continuous trickle bed reactors, and operate under O_2 pressure at temperatures of 25 to 95°C in aqueous alkaline solutions. Functional group reactivity of substrates (ketone > 1,2-diol > primary alcohol) over these oxide catalysts closely follows that reported previously when these oxides are used as anodic electrocatalysts suggesting common surface intermediates. Trickle bed reactor operation provides the highest product selectivity: *trans*-1,2-cyclohexanediol is oxidatively cleaved to adipate in NaOH solutions with 74 to 95% selectivity at contact times of 0.042 to 0.784 hr and temperatures of 26 to 95°C. The bismuth-containing oxides, $Bi_{2+x}Ru_{2-x}O_{7-y}$, show stable catalyst performance under trickle bed reactor operation for over 180 hr. Complete details of these catalytic oxidations are provided along with a discussion of substrate reaction pathways and oxygen activation by these novel expanded lattice ruthenium pyrochlore oxide catalysts.

INTRODUCTION

Ether polycarboxylates represent a large class of organic molecules useful in the sequestration of calcium and magnesium ions for detergent builder applications (*1*). If various carbohydrate molecules are to serve as substrates for the conversion to ether polycarboxylates, then a key step in this conversion is the oxidative cleavage of vicinal diols to dicarboxylate functional groups. One of the oxidation products derived from α-methyl-D-glucoside (MG) is a tricarboxylate species that bears a close resemblance to the ether tricarboxylate molecule, carboxymethyltartronate, a known organic "builder" (*1*). The oxidation of 1,2-diols to ketones (R^1, R^2, R^3, R^4 = alkyl, aryl) and aldehydes (R^1 or R^2 = H and R^3 or R^4 = H) proceeds according to Eq. (1) in which $\frac{1}{2}O_2$

[1] Current address: Monsanto Chemical Company, Rubber and Process Chemicals, Mail Zone Q4E, St. Louis, MO 63167.

[2] Current address: University of Missouri—St. Louis, Department of Physics, St. Louis, MO 63121.

[3] Current address: Monsanto Chemical Company, Advanced Performance Materials, Technology, Mail Zone Q1C, St. Louis, MO 63167.

0021-9517/91 $3.00

represents in general an electron acceptor.

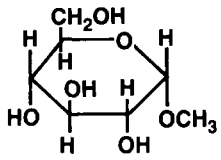

α-Methyl-D-Glucoside (MG)

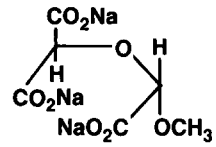

Tricarboxylate Derived from MG

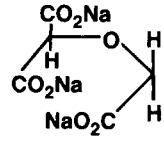

Trisodium Carboxymethyltartronate

The aldehyde intermediates may be further oxidized to carboxylic acids under suitable reaction conditions.

Stoichiometric reagents for 1,2-diol cleavage include various oxidants derived from iodine (*2–9*), lead (*3, 5, 7–10*), and bismuth (*11–16*); nitric acid, either alone or in combination with VO_2^+ (*17*); chromium(VI) oxide (*18–20*); manganese(III) pyrophosphate (*3*); nickel(III) peroxide (*21, 22*); molybdenum(VI) dioxo-bis(acetylacetonate), $MoO_2(acac)_2$ (*23*); silver(I) oxide (*24*); and cerium(IV) salts (*25*). A compilation of some of these and additional oxidants has been published (*26*). Catalytic systems for diol cleavage have been developed that use a reoxidant but function through intermediate complexes in which a variable valence state ion is cycled through high and low valence states, often differing by two valence state units. Examples of such systems include $VO_2^+/(CH_3)_3COOH$ (*27*), $FeCl_3/H_2O_2$–CH_3CN (*28*), $MoO_2(acac)_2/(CH_3)_3COOH$ (*23*), RuO_4/OCl^- (*29*), Ag^{2+}–$Ag^{3+}/S_2O_8^{2-}$ (*30, 31*), $2WO_4^{2-}$–PO_4^{3-}/H_2O_2 (*32*), and $Bi(C_6H_5)_3$ / CO_3^{2-}(aq) / *N*-bromosuccinimide (*16*). As an alternative to the use of various reoxidants, electrochemical systems have also been devised for the oxidative cleavage of 1,2-diols that include the use of carbon anodes (*33*), nickel(III) peroxide anodes (*34*), RuO_4/RuO_2–Cl^+/Cl^- with platinum electrodes (*35*), and a series of Teflon-bonded $A_{2+x}Ru_{2-x}O_{7-y}$ anodes, where A = Pb, Bi; $0 < x < 1$; and $0 < y \leq 0.5$ (*36–38*).

Competent catalytic systems for vicinal diol cleavage that make use of molecular oxygen to regenerate the reduced catalyst are relatively rare. Metalloenzymatic systems for 1,2-diol cleavage require coreductants for dioxygen apart from the active metal center as in the case of the non-heme *myo*-inositol oxygenase (*39*) and the heme cytochrome P-450_{scc} oxygenase (*40*) systems. Metal porphyrin synthetic analogue complexes of cytochrome P-450 have demonstrated 1,2-diol cleavage with the use of appropriate dioxygen coreductants (*41–43*). Inorganic analogs of these enzymatic systems that function directly with molecular oxygen are limited to soluble cobalt complexes (*44–50*) and perhaps, powdered bulk

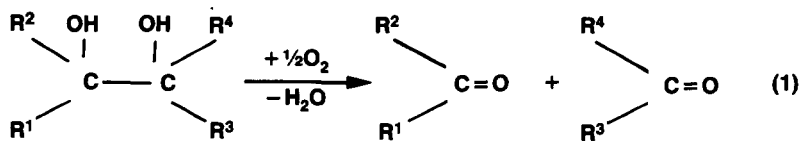

(1)

silver catalysts (*51*). The cobalt catalysts function at temperatures above 100°C, are adversely affected by the presence of water (*44*), and in some instances, do not lead to 1,2-diol cleavage products (*52*).

The present work grew out of a program to identify and develop new catalyst systems for low-temperature oxidations with molecular oxygen. Specifically, catalytic activity toward the oxidative cleavage of aqueous solutions of carbohydrate molecules that contained vicinal diol functional groups was sought. In order to simplify analytical methods development and quantitation of the reaction products, the model compound, *trans*-1,2-cyclohexanediol (TCD), was selected as a substrate for initial investigation. Because of the involvement of high-valent metal complexes in mediating vicinal diol cleavages (*16, 23, 27–32*), attention was directed toward metal oxide systems. After some preliminary experiments with the soluble heteropolymolybdate complex anion $PMo_{12}O_{40}^{3-}$ (*53*) that demonstrated qualitatively the oxidative cleavage of TCD to adipic acid at 55°C in the presence of hydrogen peroxide, efforts were made to synthesize (*54–57*) and test the catalytic activity of some expanded lattice ruthenium pyrochlore oxides (*36–38*) toward oxidative cleavage of TCD in aqueous solution using molecular oxygen. Previous reports of catalytic activity for the ruthenium pyrochlore oxides are limited to reduction of gaseous nitric oxide to dinitrogen (*58, 59*). However, several studies have used the electrically conducting ruthenium pyrochlore oxides as electrochemical electrodes to mediate chlorine evolution (*60*), hydrogen production through water electrolysis using carbohydrate feedstocks (*61*), oxygen reduction (*62–65*), and olefin oxidation (*65*). None of these studies gave any indication that it was possible to perform catalytic oxidations with the ruthenium pyrochlore oxides directly with molecular oxygen. In the first of two parts, this work describes experiments that demonstrate that the expanded lattice ruthenium pyrochlore oxides are indeed effective catalysts for the aerobic carbon–carbon bond cleavages of 1,2-diols, ketones, and olefinic linkages to produce dicarboxylate-containing molecules, as well as the aerobic oxidations of primary alcohols to carboxylates and secondary alcohols to ketones. Results from both batch autoclave and trickle bed reactors show that the catalytic oxidation activity of these oxides is a function of both the bulk composition of the ruthenium pyrochlore oxide and the identity of the organic substrate. Characterization of the ruthenium pyrochlore oxide catalyst surface composition, structure, and reactivity is the subject of an accompanying paper (*66*). Portions of this work were presented in a preliminary communication (*67*).

EXPERIMENTAL

Materials. All chemicals used in catalyst preparations and catalytic reactions and analysis were reagent grade and used as received. A sample of *cis*-1,2-cyclohexanediol (CCD) was obtained as a gift from Dr. B. L. Haymore (*68*) who followed a procedure for its preparation similar to one now published (*69*). Ruthenium nitrate was obtained as solutions from Engelhard, Strem, and Platina in which the ruthenium content (typically, 7 to 9 wt% as Ru) was determined through inductively coupled argon plasma/atomic emission spectroscopy (ICP/AES, vide infra). A sample of lead ruthenate was purchased from W. C. Heraeus and found through X-ray powder diffraction (XRD) data to contain a mixture of $Pb_2Ru_2O_{6.5}$ and RuO_2. The low surface area (vide infra) of this powder suggests that a high-temperature calcination procedure was used for its preparation.

Ruthenium pyrochlore oxide preparations. With the exception of the commercial lead ruthenate sample described above, all ruthenium pyrochlore oxides were prepared following a detailed published synthesis procedure (*57*). Details on the crystallization conditions appear in Table 1. All but one of the bismuth ruthenate samples were pre-

TABLE 1

Synthetic and Surface Area–Pore Volume Data for Various Ruthenium Pyrochlore Oxides

Formula[b]	Crystallization conditions[a]					Surface area (m^2/g)[f]	Pore volume (cm^3/g)[g]	Average pore diameter (Å)
	a (Å)[c]	M/Ru[d]	[KOH]	Time (hr)	T (°C)[e]			
$Pb_{2.63}Ru_{1.37}O_{6.5}$	10.476	2.41	6.39	162	75	52.3	—	—
$Pb_{2.62}Ru_{1.38}O_{6.5}$ (Prep. 1)[h]	10.473	2.41	7.50	161	75	60.2	—	—
$Pb_{2.62}Ru_{1.38}O_{6.5}$ (Prep. 2)	10.472	2.41	8.57	159	75	44.8	0.199	256
$Pb_{2.15}Ru_{1.85}O_{6.5}$	10.312	1.01	5.53	65	75	117.8	—	—
$Pb_{2.06}Ru_{1.94}O_{6.5}$[i]	10.283	1.00	0.86	65	75	84.9	0.222	133
$Pb_{2.00}Ru_{2.00}O_{6.5}$[j]	10.244	—	—	—	—	0.11	—	—
$Bi_{2.86}Ru_{1.14}O_{7-y}$	10.552	1.52	6,3[k]	158	85	128.0	0.312	173
$Bi_{2.46}Ru_{1.54}O_{7-y}$	10.434	1.00	9,6,3[k]	65	85	165.3	0.243	70.0
$Bi_{2.39}Ru_{1.61}O_{7-y}$	10.415	1.00	9,6,3[k]	65	85	152.3	—	—
$Bi_{2.30}Ru_{1.70}O_{7-y}$	10.390	1.00	2.1	168	85	140.6	—	—
$Bi_{1.14}Pb_{1.04}Ru_{1.82}O_{7-y}$[l]	10.383	1.00	7,6,3[k]	116	85	134.0	0.284	80.0

[a] Pure oxygen was bubbled through the slurry at about 400 cm^3/min.

[b] Derived from analysis of the X-ray powder diffraction peak positions from which the unit cell constant a was obtained.

[c] Unit cell constant for the pyrochlore crystal structure.

[d] Molar ratio of M (Pb or Bi)-to-Ru in the initial nitrate salt solution.

[e] T = temperature in degrees centigrade of the alkaline slurry during crystallization.

[f] Single point BET surface area.

[g] Pore volume distributions from which the average pore diameters were calculated.

[h] One of two preparations made that had the same formula.

[i] No oxygen was bubbled through this sample throughout the crystallization period.

[j] Commercially obtained sample.

[k] Preparation used these different KOH concentrations, each separated by a filtration step, throughout the crystallization period.

[l] Mixed bismuth and lead preparation with initial molar ratios (Bi + Pb)/Ru = 1.00. Formula was derived by elemental analysis.

pared using variations of a procedure cited in an Exxon patent (*55*) in which decreasing concentrations of KOH were used over the course of the total crystallization period. A mixed Bi–Pb ruthenium pyrochlore oxide was formed using equimolar amounts of the bismuth and lead nitrate salts dissolved in acidic $Ru(NO_3)_3$ solution. The formula for this mixed Bi–Pb ruthenium oxide was derived through Bi, Pb, and Ru elemental analyses. Additional data on the catalyst syntheses are recorded in the body and footnotes of Table 1. All ruthenium pyrochlore oxide samples were isolated as black solids that were rinsed free of excess base (phenolphthalein test) with hot water then dried in a vacuum oven at 90–100°C prior to further use. The isolated solids were readily ground and sieved to self-supporting granules of 40 to 60 mesh with good mechanical stability for trickle bed reactor operation as well as fine (below 325 mesh) powders for autoclave reactor operation and characterization studies (*66*).

Physical measurements. Elemental analyses were obtained through Galbraith Laboratories, Knoxville, TN, or at the Physical Sciences Center (PSC) at Monsanto in St. Louis, MO. The PSC analyses were acquired using a Perkin–Elmer 5500 spectrometer employing inductively coupled argon plasma/atomic emission spectroscopy (ICP/AES) techniques.

Powder X-ray diffraction (XRD) data

were collected on all of the ruthenium pyrochlore oxides reported in this work. XRD data were acquired using a Scintag PAD II system with CuK_α radiation, a high purity germanium detector maintained at 77 K, and a single channel analyzer. Published plots (*38, 56*) of a linear relationship between the cubic pyrochlore unit cell parameter, a, and the expanded lattice substitution parameter, x, in the general formula $A_{2+x}Ru_{2-x}O_{7-y}$ $(0 < x < 1, 0 < y \leq 0.5)$ produced the following relationships:

$$A = \text{Pb}: \quad x = 2.945a - 30.222$$

$$A = \text{Bi}: \quad x = 3.436a - 35.395.$$

The cubic lattice parameters (a in Table 1) were obtained from linear least-squares fits to several of the indexed reflections observed in the powder XRD patterns. The values of x were calculated from the appropriate equation above and used to generate the compositional formulas reported in Table 1 and throughout this work.

Single-point BET surface areas were measured on a Quantachrome Quantasorb instrument for all of the samples listed in Table 1. Pore volume distributions were acquired for some of the samples listed in Table 1 on a Micromeritics Digisorb 2500 instrument (PSC). Measurements on both of these instruments were periodically checked with reference materials.

Catalytic reaction products were identified through GC/MS analysis of the silylated derivatives on an automated Finnigan ei/ci mass spectrometer (PSC) preceded by a Varian 3700 gas chromatograph.

Computer graphics were used to study relationships between a surface of the lead ruthenate pyrochlore lattice and the geometry of the 1,2-cyclohexanediol isomers. The Chem-X software package (Chemical Design, Ltd., Mahwah, NJ) was used on a Lundy S5688 color graphics workstation linked to a VAX 11/780 computer (PSC).

Reactor systems and analytical methods. Preliminary examination of catalysts for the oxidative cleavage of *trans*-1,2-cyclohexanediol was conducted using a batch autoclave reactor system which has been previously diagrammed and described (*70*). This reactor system was modified for some of the catalytic oxidations in this work through the addition of a small O_2 gas reservoir and a differential pressure transducer system that afforded monitoring of O_2 gas uptakes throughout the catalytic oxidation. Figure 1 provides a schematic diagram of this modified batch autoclave reactor system.

Various catalyst compositions were evaluated using the following general procedure. A solution of 6.0 g TCD in 100 g of 1.5 *N* NaOH was charged to the autoclave containing a known amount of catalyst. The autoclave was then sealed, pressurized with O_2, vented, and pressurized to the desired operating pressure (207 or 689 kPa O_2). Reactions conducted at ambient temperature (25°C) were begun at this point (reaction time = 0.0 hr). For higher temperatures, the autoclave was first heated to the desired value prior to O_2 pressurization and reaction time initiation.

The trickle bed reactor data were obtained with a reactor system manufactured by Xytel Corporation. A schematic diagram of the relevant components appears in Fig. 2. A three-zone Applied Test Systems furnace (12-in overall heating zone with three 4-in zones) was used to heat the reactor. Machined aluminum half cylinders provided thermal contact between the furnace and the reactor tube. Samples were taken periodically from a downstream reservoir; therefore, the reactor required operation for sufficient lengths of time in order to purge the lines and reservoir of liquid from previous samples. The reactor was operated with a downflow feed of both liquid substrate solution and oxygen gas. The liquid–gas mixing occurred outside of the reactor. This mixture was introduced through a $\frac{1}{16}$-in tube to the top of the reactor bed. The liquid substrate solution was delivered by an Isco model 314 high-pressure metering pump which was calibrated over the operating

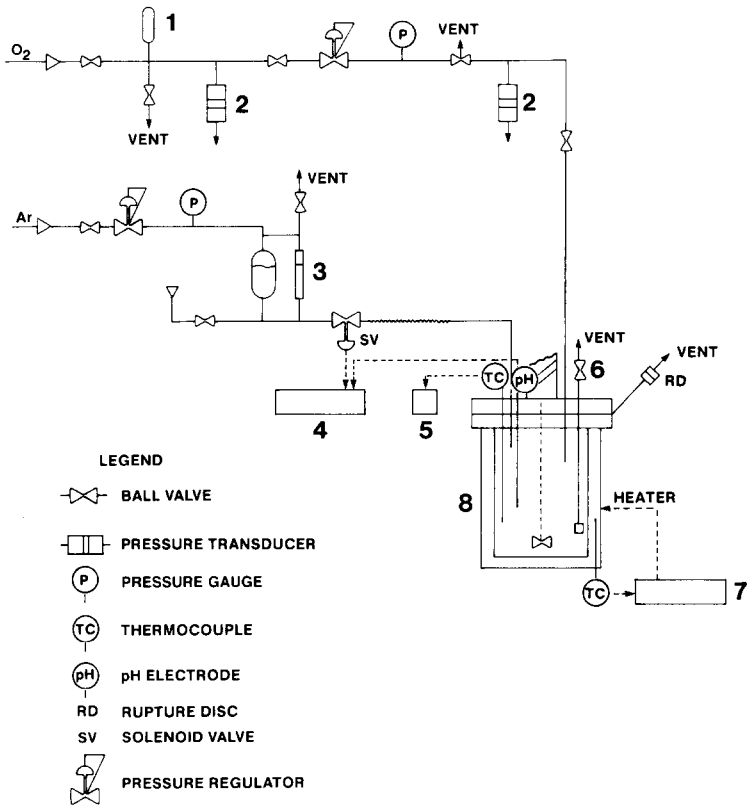

FIG. 1. Schematic drawing of the autoclave reactor system configured to evaluate the catalysts listed in Table 3. Numbered components are as follows: (1) small gas reservoir used for O_2 uptake measurement; (2) Validyne differential pressure transducer model DP15 with 0 to 3447 kPa range and read by a Validyne digital transducer indicator model CD223; (3) optional liquid feed system; (4) optional pH controller system; (5) temperature readout box; (6) sampling valve with 15-μm filter; (7) temperature controller; and (8) Autoclave Engineers 316 stainless steel 300-ml Magnedrive autoclave.

range from 0.008 to 200 ml/hr. The catalyst was located between two zones of 0.12- to 0.18-mm glass beads previously calcined at 400°C. The bottom zone was supported on a 20-μm stainless-steel fritted disc. Varying amounts of catalyst were located between the glass beads. The exact amounts are given in the tables of trickle bed reactor data (Tables 4 and 5, vide infra) for any particular catalyst loading. The reactor was constructed from $\frac{1}{4}$-in stainless-steel tubing containing a glass inner liner (Scientific Glass Engineering GLT tubing) with a 3.2-mm inside diameter. The catalyst was sieved to 40–60 mesh (0.250- to 0.373-mm particles) so that the reactor diameter (3.2 mm)-to-catalyst particle diameter ratio averaged about 10, in line with published guidelines (*71*, *72*) to avoid reactor wall effects.

A quantitative GC analytical method was developed for the analysis of *trans*-1,2-cyclohexanediol; 1,6-hexanediol; and adipic acid. Semiquantitative analysis was available for *cis*-1,2-cyclohexanediol; glutaric acid; succinic acid; maleic acid; malonic acid; and oxalic acid. The method followed the internal standard procedure (*73*) with xylitol used as the internal standard.

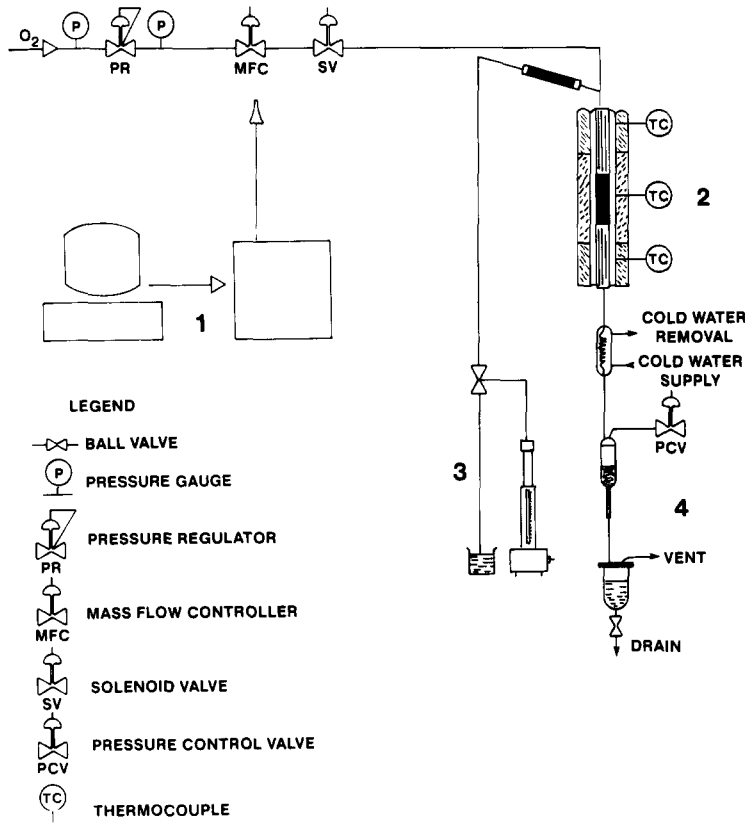

FIG. 2. Schematic diagram of trickle bed reactor system for continuous substrate oxidations. The reactor system was obtained from Xytel Corporation and has the following numbered components: (1) DEC VT100 terminal with Intel 8086 cpu microcomputer and Analog Devices interface; (2) three-zone Applied Test Systems furnace and reactor consisting of 3.2-mm-id (1/4 in od) stainless-steel tubing with glass inner liner (SGE GLT tubing); (3) Isco model 314 high pressure liquid metering pump feeding 0.008 to 200 ml/hr; and (4) liquid sample reservoir.

Sample analysis was typically performed in duplicate according to the following procedure. The aqueous alkaline (typically, NaOH) solution was transferred as a 100-μl aliquot to a GC sample vial and acidified with 100 μl of 1.5 *N* HCl. The sample mixture was then evaporated to dryness under a nitrogen gas stream in a hood. The solid residue (typically composed of diols, sodium carboxylate salts, and NaCl) was then derivatized in a 100-μl volume of pyridine containing the xylitol standard with Regis RC-3 reagent [bis(trimethylsilyl)trifluoroacetamide containing 10% trimethylchlorosilane, about 0.3 ml] by heating the capped vial at 100°C for 30 min. Aliquots of 0.2 μl were injected onto a methyl silicone capillary column (HP 190952, No. 121) in a Hewlett–Packard 5710A gas chromatograph equipped with flame ionization detection using an HP 5704A electrometer module. The GC was programmed as follows: 100–250°C at 8°C/min with an 8-min hold at 250°C.

The oxidation of aqueous 2-butanol to 2-butanone was followed using carbon-13 NMR spectroscopy. Samples at various reaction conditions and times were recovered from the trickle bed reactor. Aliquots were loaded into a 10-mm NMR tube into which was inserted a coaxial inner cell containing

dimethyl-d_6 sulfoxide as an external standard. NMR data were acquired using a Varian XL 200 spectrometer.

RESULTS

As can be seen in Table 1, 10 of the 11 ruthenium oxides listed were prepared by low-temperature alkaline precipitation and crystallization (*57*). One ternary ruthenium oxide in Table 1, denoted as $Pb_{2.00}Ru_{2.00}O_{6.5}$, was secured from a commercial vendor. This sample is representative of a ruthenium pyrochlore oxide prepared by conventional high-temperature ceramic methods. The 10 solution-crystallized mixed ruthenium oxides were found from powder X-ray diffraction data to be single phase compounds having the pyrochlore structure type. Formulas for the lead and bismuth ruthenium oxides were obtained by the linear relationships given in the Experimental section between the lattice expansion parameter x in the general formula $A_{2+x}Ru_{2-x}O_{7-y}$ and the cubic pyrochlore cell constant as derived from the powder XRD patterns. Representative XRD patterns for four of the ruthenium pyrochlore oxides are displayed in Fig. 3. Although all four compounds show broad X-ray diffraction line widths, within this series the lead ruthenium oxides, shown in tracings A and B in Fig. 3, show relatively sharp diffraction lines compared to the bismuth-containing ruthenium oxides in tracings C and D. Note that the mixed lead–bismuth ruthenium pyrochlore oxide in tracing D appears intermediate in its X-ray diffraction line widths to the lead ruthenium (tracings A and B) and bismuth ruthenium (tracing C) oxides.

The measured BET surface areas for these ruthenium pyrochlore oxides are recorded in Table 1. These surface areas generally follow the X-ray diffraction line widths in that the broader lines lead to compounds having higher surface areas. This is particularly true for the bismuth-containing compounds. A quantitative analysis of the X-ray diffraction line widths will be presented in the following paper (*66*) as an estimate of the average crystallite particle size of these solution-crystallized ruthenium pyrochlore oxides.

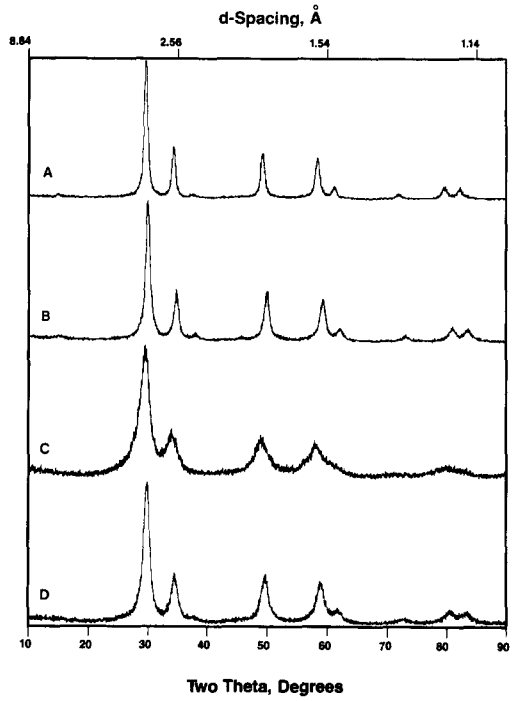

FIG. 3. Representative X-ray powder diffraction patterns for four ruthenium pyrochlore oxides reflecting variations in crystallinity and particle size: $Pb_{2.63}Ru_{1.37}O_{6.5}$ (A), $Pb_{2.15}Ru_{1.85}O_{6.5}$ (B), $Bi_{2.86}Ru_{1.14}O_{7-y}$ (C), and $Bi_{1.14}Pb_{1.04}Ru_{1.82}O_{7-y}$ (D).

Oxidative cleavage of 1,2-cyclohexanediol and cyclohexanone. Since the *trans* isomer of 1,2-cyclohexanediol represents the diol geometry encountered in naturally occurring carbohydrates such as starch, preliminary evaluations for viable diol oxidation catalysts were conducted exclusively with TCD. Selected results for batch autoclave reactor testing of below 325-mesh (44-μm) powders of $Pb_{2.62}Ru_{1.38}O_{6.5}$ for catalytic oxidative cleavage activity toward TCD are summarized in Table 2. Variations were made in these runs in the amount of catalyst, the amount of TCD substrate, the amount of alkali hydroxide base, and the reaction temperature. All catalytic reactions shown in this table were conducted with a continu-

TABLE 2

Preliminary Batch Autoclave Reactor Conditions and Results for *trans*-1,2-Cyclohexanediol (TCD) Using $Pb_{2.62}Ru_{1.38}O_{6.5}$ Catalyst[a]

Entry	Catalyst amount (g)	TCD amount (g)	[Base][b]	T (°C)	Reaction time (hr)	TCD conversion (%)	Selectivity (AA[c]) (%)
1	2.00	6.00	None[d]	55	4.0	0.0	0.0
2	2.00	6.00	3.0 NaOH	45	4.0	97.8	31.3
3	2.00	1.00	1.0 KOH	55	4.0	100.0	75.4
4	4.00	6.00	3.0 KOH	25	7.0	97.8	50.6
5	2.00[e]	6.00	3.0 KOH	25	4.0	9.6	100.0
6	4.00	7.65[f]	3.0 KOH	25	4.0	—	100.0[g]

[a] Catalytic oxidations conducted at 207 kPa O_2 pressure with an agitation rate of 1500 rpm.
[b] Concentration of 100 ml of base used; identity of base shown below initial concentration.
[c] AA = adipic acid dianion (analyzed as free acid).
[d] Initial pH 4.90 and final pH 5.45.
[e] Catalyst recycled from preceding entry, 1.60 g, to which 0.40 g of fresh catalyst were added.
[f] Amount of adipic acid charged (no TCD).
[g] No conversion of adipic acid substrate observed by analysis.

ous purge of the reactor headspace with the total oxygen pressure on the system remaining constant at 207 kPa. In addition to the small catalyst particle size, the reactions were conducted at an agitation rate of 1500 rpm to minimize mass-transfer effects from both the substrate and the oxygen gas. Previous catalytic oxidations conducted in this batch autoclave reactor system indicate that for a solution volume of 100 ml at 207 kPa O_2 pressure and 1500 rpm, oxygen mass transfer from the gas to the liquid becomes reaction-rate limiting when O_2 is consumed at a rate above about 0.1 mol O_2/hr.

Entry 1 in Table 2 shows that if no alkali hydroxide is added to the aqueous TCD substrate solution, no conversion occurs throughout a 4-hr period when stirred with a slurry of 2.0 g of $Pb_{2.62}Ru_{1.38}O_{6.5}$. However, as can be seen from entry 2, when alkali hydroxide is added to the TCD substrate solution, nearly complete conversion of TCD occurs under comparable time and reaction conditions with this catalyst. Note that the amount of alkali hydroxide added is about three-to-six times over that required for stoichiometric conversion of TCD to the dicarboxylate product. GC analysis of the trimethylsilyl-derivatized reaction products produced a TCD conversion of 97.8% but a selectivity of only 31.3% to the desired adipic acid product. GC/MS analysis of the derivatized reaction mixture revealed lower diacids of the type $HO_2C(CH_2)_nCO_2H$ with n = 0, 1, 2, and 3 in addition to adipic acid (n = 4) and some monoacids with carbon chain lengths of 15, 17, and 18. Possible mechanistic routes to these observed reaction by-products are discussed in the next section.

Entries 3 through 5 in Table 2 indicate ways by which the reaction selectivity to adipic acid can be improved. As seen in entry 3, if the base concentration is lowered to 1.0 N and the amount of TCD substrate is kept low relative to the charge of catalyst (moles TCD/moles catalyst = 3.4), the selectivity to the desired adipic acid product more than doubled over that in entry 2 to a value of 75.4%. Entries 4 and 5 reflect the

effect of lower reaction temperature on the reaction selectivity. In entry 4, the reaction was run at 25°C and the selectivity to adipic acid increased to 50.6% over that for entry 2 run at 45°C. The use of less catalyst in entry 5 over that in entry 4 produced much less conversion of the TCD substrate over a 4-hr period, but the selectivity to adipic acid was essentially 100%. Entry 6 in Table 2 demonstrates that once the adipic acid product forms, it is stable toward any further oxidation. Overall, the preliminary runs in Table 2 suggest that $Pb_{2.62}Ru_{1.38}O_{6.5}$ is effective for the catalytic oxidative cleavage of TCD. Higher selectivity to adipic acid product is achieved if the reaction temperature (25°C over 45–55°C), the substrate-to-catalyst ratio, and the alkali hydroxide concentration are all kept relatively low.

On the basis of the initial results presented in Table 2, the autoclave reactor was modified with the addition of a pressure transducer system as depicted in Fig. 1. This pressure transducer system affords semiquantitative oxygen gas uptakes for any reaction time. Although the autoclave reactor was equipped with liquid sampling valves, the progress of a "new" catalytic oxidation was best measured by the rate of oxygen uptake. Since liquid samples require derivatization and GC analysis before conversion-selectivity data are available, the oxygen uptake values provide a more immediate indicator of the relative reaction rate and overall progress of the reaction. Oxygen gas uptake data were particularly useful in establishment of a suitable reaction temperature to conduct the catalytic oxidation and in determination of when the endpoint of the reaction was reached.

Table 3 assembles data from eight different catalytic oxidations with variations in the catalyst composition and substrate represented. All runs were conducted under similar conditions: 4.00 g of ruthenium pyrochlore catalyst, 6.00 g of substrate dissolved in 1.5 *N* NaOH, 689 kPa O_2, and a stirring rate of 1500 rpm. Reactions were generally performed at the lowest possible reaction temperature necessary to sustain a reasonable uptake of O_2 (about 100 kPa/hr). On the basis of a total system volume of about 160 cm^3, the calculated oxygen uptake was related approximately to the number of moles of O_2 reacted according to the reaction stoichiometry through a factor of 15500 kPa O_2/mole. For the catalytic oxidation of TCD the reaction stoichiometry was assumed to be

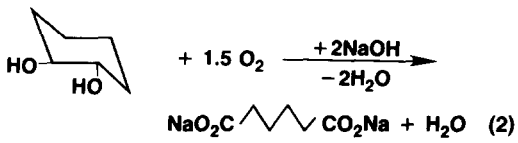

(2)

In the case of entry 1 in Table 3, 0.0517 moles of TCD substrate require 0.0776 moles of O_2 for complete conversion to adipic acid product. The observed uptake of 1110 kPa O_2 agrees to within 92% of the calculated value of 1201 kPa O_2. However, the calculated value does not account for the additional oxygen required as a result of by-product formation. The other entries in Table 3 did not show such close agreement between the calculated and observed O_2 uptakes. Accordingly, all conversion-selectivity calculations were based on the GC analytical values.

In addition to the analytical results providing conversion-selectivity data, Table 3 gives substrate/catalyst ratios for the batch reactions. All of these ratios were around 10 for the reactions examined here. The catalytic oxidations again used 44-μm powders of the various catalyst compositions. As can be seen from the reaction times, all reactions proceed relatively slowly, indicative of operation in the reaction-rate limiting regime. As noted above for this particular reactor, oxygen mass-transfer effects will occur if the reaction consumes greater than 0.1 mole O_2/hr or 1550 kPa O_2/hr. Examination of the reaction times shows that only the cyclohexanone substrate in entry 8 *approaches* this oxygen mass-transfer-limiting regime with 0.0856 mole/hr of substrate converted.

As an index of the relative catalytic activity for each of the catalysts, two quantities

TABLE 3

Representative Batch Autoclave Reactor Conditions and Results for 1,2-Cyclohexanediol, Cyclohexanone, and 1,6-Hexanediol Catalytic Oxidations[a]

Entry	Catalyst	Substrate (g)[b]	T (°C)	Reaction time (hr)	O_2 Uptake (kPa)	Substrate conversion (%)	Selectivity (AA[c]) (%)	Substrate/ catalyst molar ratio	PROD[d]	Specific activity[e]
1	$Pb_{2.62}Ru_{1.38}O_{6.5}$	6.00(TCD)	25	7.0	1110.	100.0	71.7	10.2	1.04	0.0220
2	$Pb_{2.62}Ru_{1.38}O_{6.5}$	6.00(CCD)	25	4.0	951.	98.5	74.6	10.2	1.87	0.0395
3	$Pb_{2.15}Ru_{1.85}O_{6.5}$	6.00(TCD)	25	7.2	434.	45.4	57.7	9.5	0.35	0.0040
4	$Pb_{2.00}Ru_{2.00}O_{6.5}$	6.00(TCD)	35	1.0	0.	11.0	0.0	9.3	0.00	0.0000
5	$Bi_{2.46}Ru_{1.54}O_{7-y}$	6.00(TCD)	40[f]	6.3	662.	70.0	99.6	10.1	1.12	0.0087
6	$Bi_{1.14}Pb_{1.04}Ru_{1.82}O_{7-y}$	6.00(TCD)	55	5.3	996.	98.8	76.8	9.3	1.34	0.0138
7	$Pb_{2.62}Ru_{1.38}O_{6.5}$	6.00(CHO)	35[g]	1.4	1007.	100.0	68.9	12.0	5.91	0.125
8	$Pb_{2.63}Ru_{1.37}O_{6.5}$	6.00(HD)	55[h]	6.0	951.	100.0	57.0	10.0	0.95	0.0232

[a] Catalytic oxidations conducted with 4.00 g catalyst in 100-ml 1.5 *N* NaOH, at 689.5 kPa O_2 pressure, and with an agitation rate of 1500 rpm.
[b] Codes for substrates: TCD = *trans*-1,2-cyclohexanediol; CCD = *cis*-1,2-cyclohexanediol; HD = 1,6-hexanediol; CHO = cyclohexanone.
[c] AA = adipic acid dianion.
[d] PROD = productivity = Moles of substrate reacted selectively to product in one hour/moles catalyst.
[e] Specific activity = millimoles of substrate reacted selectively to product in 1 hr/m^2 catalyst surface.
[f] Initial temperature of 25°C produced no O_2 uptake so temperature was increased to 40°C.
[g] Average temperature for reaction time period after starting at 25°C.
[h] Initial temperature of 25°C produced only 10.3 kPa O_2 uptake in 30 min, so temperature was increased to 55°C for the remainder of the run.

are used that appear in the last two columns of Table 3. The productivity of the catalysts, PROD, is defined, with slight modification to that used before (*75*), by

$$\text{PROD} = \frac{\text{Mol of substrate reacted selectively to product}}{(\text{Mol of catalyst})(\text{hr})} \quad (3)$$

The specific activity is tabulated in the last column of Table 3 in order to place all of the catalysts on the same scale with respect to their available surface area. The specific activity is defined by

$$\text{Specific Activity} = \frac{\text{Millimol of substrate reacted selectivity to product}}{(\text{m}^2 \text{ of catalyst surface})(\text{hr})} \quad (4)$$

where the catalyst surface is measured by the BET N_2 surface area recorded in Table 1.

Entries 1 and 2 in Table 3 provide a direct comparison of the geometrical isomer effects of 1,2-cyclohexanediol on the oxidative cleavage rate by the same lead ruthenium pyrochlore oxide catalyst composition. The *cis* isomer examined in entry 2 is essentially completely converted to product in 4 hr, while the *trans* substrate in entry 1 requires 7 hr to achieve complete conversion of the same amount of substrate. Oxygen uptake rates were monitored for both reactions and at one point the O_2 uptake rate for CCD exceeded more than twice that observed for TCD. The *cis* isomer produced adipic acid in slightly higher selectivity (75%) than the *trans* substrate (72%).

The relatively high lead content in the Pb–Ru pyrochlore oxide catalysts appears beneficial for 1,2-diol oxidative cleavage activity. Entry 3 of Table 3 shows that for the relatively low lead-containing catalyst, $Pb_{2.15}Ru_{1.85}O_{6.5}$, a TCD conversion of only 45% is obtained over a 7-hr period with much poorer selectivity to adipic acid than either TCD or CCD substrates with $Pb_{2.62}Ru_{1.38}O_{6.5}$. This result appears rather unexpected in light of the much higher surface area for $Pb_{2.15}Ru_{1.85}O_{6.5}$ (118 m^2/g) compared to that found for the $Pb_{2.62}Ru_{1.38}O_{6.5}$ catalysts (45 to 60 m^2/g). Surface characterization results presented in the following pa-

per (*66*) suggest possible origins for superior oxidative cleavage activity by the higher Pb/Ru ratio oxide catalysts. The commercial $Pb_{2.00}Ru_{2.00}O_{6.5}$ catalyst in entry 4 with an exceedingly low surface area as well as a low Pb/Ru ratio produced no O_2 uptake over a 1-hr period even after raising the reaction mixture to 35°C. GC analysis of the recovered reaction solution showed no adipic acid was produced with about 11% of the TCD converted to unidentified products.

The structural and electronic effects caused by substitution of bismuth for lead in the ruthenium pyrochlore oxides were probed in the evaluation of $Bi_{2.46}Ru_{1.54}O_{7-y}$ for the oxidative cleavage of TCD in entry 5, Table 3. In contrast to the lead analogs in entries 1 through 3, no oxygen uptake was detected at a reaction temperature of 25°C. However, when the autoclave was heated to 40°C, O_2 uptake commenced and continued at a steady rate for more than 6 hr. At this point the reaction was stopped and the solution recovered from the $Bi_{2.46}Ru_{1.54}O_{7-y}$ catalyst by filtration. Analysis of solution aliquots showed a TCD conversion of 70% with a surprisingly high selectivity to adipic acid product of essentially 100%. As with all analyses, this analytical result was run in duplicate and the results averaged to confirm the unusually high selectivity. Inspection of the PROD value for $Bi_{2.46}Ru_{1.54}O_{7-y}$ shows a value of 1.12, a number higher than that for the $P_{2.62}Ru_{1.38}O_{6.5}$ catalyst in entry 1 (1.04). Because this catalyst has a relatively high surface area, the specific activity is only about one-third that observed for the Pb–Ru catalyst in entry 1. These results point out the distinct catalytic behaviors of the Pb–Ru and Bi–Ru catalysts toward the oxidative cleavage of TCD.

Mixed bismuth– and lead-ruthenium pyrochlore oxides can be prepared over a wide solid solution range. One such mixed bismuth–lead ruthenium oxide with the empirical formula $Bi_{1.14}Pb_{1.04}Ru_{1.82}O_{7-y}$ is found to catalyze the oxidative cleavage of TCD in a manner similar to that of the lead and bismuth analogs with slightly higher selectivity to adipic acid compared to an all-lead analog. However, a temperature of 55°C was required with this mixed Bi–Pb–Ru oxide in order to produce a reasonable rate of reaction as judged by O_2 uptake values. In contrast to some of the preliminary runs recorded in Table 2, this particular catalyst afforded good selectivity to adipic acid in spite of the relatively high reaction temperature.

Cyclic ketones such as cyclohexanone (CHO) are also oxidatively cleaved by ruthenium pyrochlore oxide catalysts. Entry 7 in Table 3 provides details on one such batch autoclave oxidation. Although the oxidation was begun at only 25°C with the same substrate charge as used for the 1,2-diol substrates, the rate of O_2 uptake was exceedingly rapid. Here for the first time, the oxidation rate produced an observable temperature rise in the reaction mixture (no external heating) from 25°C up to about 40°C. The average temperature throughout the 1.4-hr reaction time was 35°C. This oxidative cleavage was complete in less than half the time for a 1,2-diol substrate. GC analysis showed complete conversion of the CHO substrate. The selectivity to adipic acid was markedly lower than those observed with the 1,2-diol substrates with the same catalyst, perhaps due in part to the uncontrolled temperature excursion throughout the reaction period. Possible reaction mechanisms to account for the high oxidation activity of the CHO substrate are considered in the Discussion section.

Laboratory trickle bed reactor data were initially sought as a means by which to decrease the substrate/catalyst molar ratio over that used in batch autoclave reactor operation with the aim of increasing the overall reaction selectivity in the TCD to adipate conversion. Additionally, a trickle bed reactor provides a means for continuous operation from which information on longer-term catalyst stability can be obtained. Using the reactor system shown in the diagram in Fig. 2, data were obtained according to the reactor and catalyst size guidelines

TABLE 4

Continuous Trickle Bed Reactor Data for *trans*-1,2-Cyclohexanediol and 1,6-Hexanediol Catalytic Oxidations[a]

Entry	Substrate[b]	T (°C)	Contact time (hr)[c]	Substrate conversion (%)	(No.)[d]	Selectivity (%)[e]	Substrate/ catalyst[f] molar ratio	PROD[g]	Specific activity[h]
				A. $Pb_{2.63}Ru_{1.37}O_{6.5}$, 4.69 g, 3.92 cm^3					
1	TCD	26	0.784	100.0	(8)	88.0	0.43	0.38	0.0092
2	TCD	55	0.261	99.8	(12)	85.6	1.3	1.11	0.0270
				B. $Bi_{2.39}Ru_{1.61}O_{7-y}$, 3.60 g, 3.10 cm^3					
3	TCD	45	0.620	99.4	(4)	89.1	0.56	0.49	0.0042
4	TCD	55	0.620	100.0	(2)	94.9	0.56	0.53	0.0045
5	TCD	55	0.310	100.0	(2)	88.1	1.1	0.98	0.0083
6	TCD	55	0.207	99.7	(2)	86.8	1.6	1.39	0.0118
7	HD	55	0.620	98.1	(6)	90.8	0.56	0.49	0.0042
8	HD	75	0.207	100.0	(4)	87.7	1.6	1.44	0.0122
9	HD	75	0.155	100.0	(2)	87.7	2.2	1.92	0.0162
10	HD	95	0.155	100.0	(2)	85.2	2.2	1.86	0.0158
11	HD	95	0.124	100.0	(4)	85.3	2.7	2.38	0.0202
12	HD	95	0.089	100.0	(2)	85.9	3.8	3.28	0.0278
14	HD	95	0.078	100.0	(2)	83.8	4.4	3.66	0.0310
15	HD	95	0.062	100.0	(2)	91.3	5.5	4.98	0.0423
				C. $Bi_{2.86}Ru_{1.14}O_{7-y}$, 3.27 g, 3.10 cm^3					
16	TCD	95	0.055	100.0	(2)	81.0	7.3	5.91	0.0560
17	TCD	95	0.042	65.2	(2)	74.2	9.6	4.67	0.0442

[a] Performed in 3.2-mm-id glass-lined tubing as a reactor containing 40–60 mesh (0.373–0.250 mm) catalyst granules packed between 0.12- and 0.18-mm glass beads with ca. 0.5 *M* substrate in 1.5 *N* NaOH, 689.5 kPa O_2 pressure, and a downflow feed of liquid substrate and 30–45 cm^3/min O_2.

[b] Codes: TCD = *trans*-1,2-cyclohexanediol and HD = 1,6-hexanediol.

[c] Contact time = volume of catalyst/volumetric substrate flow rate.

[d] Number of independent samples averaged to give the conversion–selectivity data shown.

[e] Calculated selectivity to adipic acid product.

[f] Based on catalyst reactor volume.

[g] PROD = productivity = moles of substrate reacted selectively to product in one hour/mole catalyst.

[h] Specific activity = millimoles of substrate reacted selectively to product in 1 hr/m^2 catalyst surface.

and operation presented in the Experimental section.

Table 4 presents a selected summary of trickle bed reactor data collected on three different catalysts for the oxidative cleavage of TCD in 1.5 *N* NaOH. This table is divided into three sections (A–C) which represent different $A_{2+x}Ru_{2-x}O_{7-y}$ catalyst compositions. For each catalyst listed, the amount and volume occupied by the 40 to 60 mesh granules are given. The volume recorded is that occupied by the granules including solid and void volumes. Temperatures recorded in Table 4 represent those at the reactor inlet. As noted elsewhere (*76*), the reactor contact or space time does not represent an actual residence time of the reactants but is a ratio between the catalyst volume and the volumetric flow rate of substrate solution at the reactor inlet. TCD conversions and selectivities recorded for entries 1–6, 16, and 17 in Table 4 are averages over a number (no.) of independent samples taken at the reaction conditions shown. The last three

columns of Table 4 list the substrate/catalyst molar ratios, PROD values, and specific activity values. These listings offer a basis for comparison with the results obtained in Table 3 under batch autoclave reactor conditions.

As seen for the $Pb_{2.63}Ru_{1.37}O_{6.5}$ catalyst data in section A of Table 4, shorter contact times (i.e., higher volumetric flow rates) lead to slightly lower selectivity in the conversion of TCD to adipate. At a reaction temperature of 55°C in entry 2, a contact time of 0.261 hr produces a substrate/catalyst molar ratio that is about a factor of 10 lower than that in an autoclave reactor, but essentially the PROD and specific activity are the same values as those for the $Pb_{2.62}Ru_{1.38}O_{6.5}$ catalyst of entry 1, Table 3. However, the selectivity at close to 100% TCD conversion in the trickle bed reactor sample (Table 4, entry 2) approaches 86% to adipate compared to only 72% at 25°C in the batch reactor. Similarly high selectivities to adipate are observed with the $Bi_{2.39}Ru_{1.61}O_{7-y}$ catalyst in Table 4, entries 3–6. In section C of Table 4 are shown trickle bed reactor data for a $Bi_{2.86}Ru_{1.14}O_{7-y}$ catalyst run at much higher temperatures (95°C) and shorter contact times than the other Table 4 entries. For a contact time of 0.055 hr (entry 16), it is possible to achieve complete conversions of the TCD substrate while keeping the adipate selectivity (81%) higher than that obtainable in a batch reactor. Shorter contact times (0.042 hr, entry 17) produce incomplete conversion of TCD, some yellowing of the reactor effluent, and lower selectivity to adipate (74%).

Oxidation of 1,6-hexanediol. With an established analytical method for the adipic acid product, a convenient substrate to examine as a test for $A_{2+x}Ru_{2-x}O_{7-y}$-catalyzed oxidation of primary alcohol groups is 1,6-hexanediol (HD). The assumed catalyzed reaction stoichiometry is

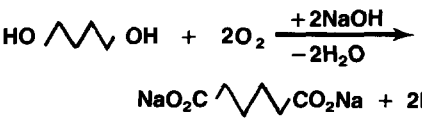

(5)

Evaluation of HD in a batch reactor with $Pb_{2.63}Ru_{1.37}O_{6.5}$ as a catalyst (entry 8, Table 3) shows that the substrate is not catalyzed identically to that of the 1,2-diol substrates at 25°C. HD requires a temperature of about 55°C to sustain an appreciable rate of conversion as judged by the O_2 uptake. The observed selectivity to adipate of only 57% suggests that this substrate might be more selectively converted under trickle bed reactor conditions as was found for the TCD substrate.

An extensive series of runs in a trickle bed reactor were made with HD substrate in 1.5 *N* NaOH solution using $Bi_{2.39}Ru_{1.61}O_{7-y}$ catalyst granules. The results of these runs are collected in Table 4, section B, entries 7–15. These nine entries encompass some 26 independent samples collected over a temperature range of 55 to 95°C with contact times spanning an order of magnitude. In essentially all entries the HD conversion is 100% with the observed selectivities to adipate ranging from 84 to 91%. These selectivities clearly point out the beneficial effect produced by the lower substrate/catalyst ratio encountered in the trickle bed reactor over that in the autoclave reactor.

Oxidation of 2-butanol to 2-butanone. Previous work that used expanded lattice ruthenium pyrochlore oxides as anodic electrocatalysts for various organic substrate oxidations (*37*) demonstrated that basic buffered solutions of secondary alcohols afforded electrochemical conversion to the two-electron oxidized ketone product. Accordingly, it was of interest to see if under oxygen pressure, the selective conversion of 2-butanol to 2-butanone would proceed using a pH 9.35 $Na_2B_4O_7$ solution. A 0.81 *M* 2-butanol solution saturated with $Na_2B_4O_7$ was passed over granules of a $Bi_{2.86}Ru_{1.14}O_{7-y}$ catalyst in a trickle bed reactor and collected at temperatures of 55 to 115°C under about 660 kPa O_2 pressure (30 cm^3/min O_2 fed downflow) at various contact times. The progress of the reaction was monitored by ^{13}C NMR spectroscopy.

The ^{13}C NMR spectrum of a representa-

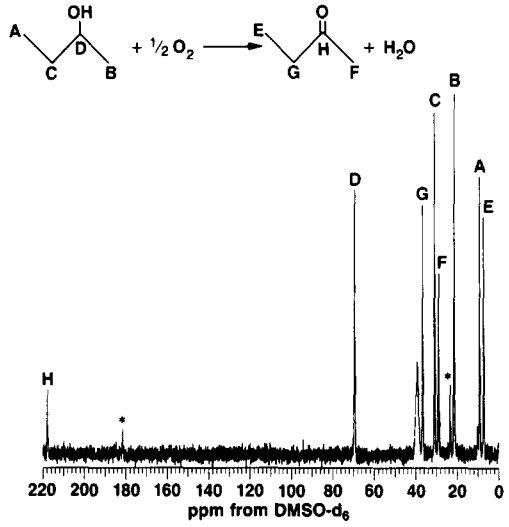

FIG. 4. Carbon-13 NMR spectrum of the reaction product obtained by passing 0.81 *M* 2-butanol in saturated $Na_2B_4O_7$ aqueous solution (pH 9.35) over a $Bi_{2.86}Ru_{1.14}O_{7-y}$ catalyst at 95°C under 662 kPa O_2 pressure with a contact time of 1.03 hr. Carbon resonances labeled A through D are associated with the 2-butanol substrate while those labeled E through H correspond to the desired 2-butanone product. A small amount of acetate by-product is indicated by the asterisks on the lines at 23.5 and 180.9 ppm. The five-line reference multiplet for DMSO-d_6 is centered around 39.5 ppm.

tive trickle bed reactor sample is displayed in Fig. 4. All of the observed resonance peaks have been assigned to either the 2-butanol substrate (A–D in Fig. 4), the 2-butanone product (E–H), the acetate by-product (* marked positions), or the DMSO-d_6 reference multiplet centered around 39.5 ppm. While this spectrum confirms that the major oxidation product is the ketone, the catalyst under these reaction conditions is not completely selective to the two-electron oxidation product as judged from the appearance of a small amount of acetate cleavage product. Based on the partial selectivity to 2-butanone and the reaction conditions under which the NMR sample was taken, reasonable estimates for PROD and specific activity values defined in Eqs. (3) and (4) are 0.3 mol 2-butanol reacted selectively to 2-butanone/mol $Bi_{2.86}Ru_{1.14}O_{7-y}$-hr and 0.003 millimol 2-butanol reacted selectively to 2-butanone/m^2-$Bi_{2.86}Ru_{1.14}O_{7-y}$-hr, respectively.

Oxidative cleavage of maleic acid. The oxidative cleavage of olefinic bonds was found to proceed electrochemically over $A_{2+x}Ru_{2-x}O_{7-y}$ anodes (*37*) under aqueous alkaline conditions. A convenient olefinic substrate that was used in the electrochemical oxidations in aqueous alkaline solution is maleic acid. The ability of an $A_{2+x}Ru_{2-c}O_{7-y}$ catalyst to mediate the oxidative cleavage of maleic acid in the presence of molecular oxygen was examined in aqueous alkaline solutions. The assumed catalytic oxygen-driven reaction proceeds according to

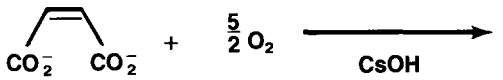

$$2\ C_2O_4^{2-} + H_2O \quad (6)$$

Trickle bed reactor data were obtained on a 0.127 *M* maleic acid substrate containing 0.67 *N* CsOH. The cesium salt was used rather than the potassium or sodium salts due to the high solubility of cesium oxalate compared to either of the other alkali salts of oxalic acid. The results on four samples taken at various contact times at 95°C over the $Bi_{2.30}Ru_{1.70}O_{7-y}$ catalyst are reported in Table 5. From the calculated substrate/catalyst ratios, the highest selectivity to oxalate product occurs at higher rather than lower ratios. This trend is not followed by any of the other catalytic oxidations in Tables 3 and 4.

Catalyst stability. In both the batch autoclave and trickle bed reactor runs listed in Tables 2 through 5, the bulk mechanical stability of the ruthenium pyrochlore oxide catalysts was adequate for repeated use. Since crystallization from hot aqueous alkaline solutions occurs for the expanded lattice ruthenium pyrochlore oxides under conditions similar to those used in the catalytic oxidations described here, it was of interest to investigate the possible presence of soluble post-transition metal and ruthenium ions. Such ions potentially may be leached from

TABLE 5

Continuous Trickle Bed Reactor Data for Catalytic Oxidation of Maleic Acid Using $Bi_{2.30}Ru_{1.70}O_{7-y}$ at 95°C[a]

Entry	Contact time (hr)[b]	Conversion (%)	Selectivity (%)[c]	Substrate/catalyst molar ratio	PROD[d]	Specific activity[e]
1	0.620	97.7	53.9	0.190	0.100	0.00093
2	0.620	100.0	58.3	0.190	0.111	0.00103
3	0.207	56.0	56.0	0.571	.179	0.00167
4	0.124	41.0	70.2	0.952	0.274	0.00255

[a] Catalyst in the form of 40 to 60 mesh granules weighing 2.55 g and occupying a reactor volume of 3.10 cm^3. The 0.127 *M* maleic acid substrate in 0.67 *N* CsOH was passed at various flow rates through the catalyst bed at 689 kPa O_2 pressure with O_2 fed along with the substrate at a rate of 30 cm^3/min.

[b] Contact time = volume of catalyst/volumetric substrate flow rate.

[c] Selectivity calculated to oxalic acid (oxalate) product.

[d] PROD = moles of maleic acid reacted selectively to product in one hour/mole of catalyst.

[e] Specific activity = millimoles of maleic acid reacted selectively to product in 1 hr/m^2 of catalyst surface.

the solid pyrochlore oxide catalyst, and therefore, these species might play a role in the observed catalytic reactions.

As seen in Fig. 3 and in the data contained in Table 1, the lead ruthenium pyrochlores develop greater crystallinity under lower alkali hydroxide strengths than do the bismuth analogs. Accordingly, the first tests for the presence of soluble ions were made on reaction product solutions using the $Pb_{2.62}Ru_{1.38}O_{6.5}$ catalyst (Table 2, entry 4 and Table 3, entry 1). ICP/AES analyses of the filtered reaction solutions revealed the presence of lead and ruthenium in concentrations averaging 1×10^{-4} and 4×10^{-8} *M*, respectively. These concentrations are somewhat below those observed (*62*) when similar $Pb_{2+x}Ru_{2-x}O_{6.5}$ compounds were used as electrochemical composite anodes in 3 *N* KOH for oxygen reduction.

The substrate-to-catalyst ratios used in all of the catalytic oxidations described here greatly exceed the stoichiometric amounts required for conversion of the substrates into the observed products. The low substrate/catalyst ratios used are a result of the intrinsically slow rate of oxidative cleavage of the 1,2-diol substrates at these low reaction temperatures and the need to convert efficiently the more reactive aldehyde intermediates to carboxylate products. Further arguments in support of the observed catalysis are given in the next section where a fuller body of evidence for genuine heterogeneous catalysis mediated by the pyrochlore oxide surfaces is considered.

Trickle bed reactor experiments were preferentially performed with the $Bi_{2+x}Ru_{2-x}O_{7-y}$ catalysts in light of the similar if not superior results produced for catalytic oxidative cleavage of TCD. The presence of soluble lead and ruthenium species found in the reaction product solutions above also pointed to the more effective use of the bismuth–ruthenium oxides in continuous reactor experiments. Table 4, section B, compiles some continuous trickle bed reactor data for a $Bi_{2.39}Ru_{1.61}O_{7-y}$ catalyst subjected to 1,2-diol and primary alcohol substrates. The total duration for these experiments spanned 3 months during which time the catalyst was on stream to substrate solutions for more than 180 hr. No evidence for catalyst deactivation was observed during this time. A 500-ml solution collected from HD oxidations at 95°C was analyzed by ICP/AES for bismuth and ruthenium. No detectable levels of these ions were observed. An XRD powder pattern comparison of the granular catalyst was made before and after

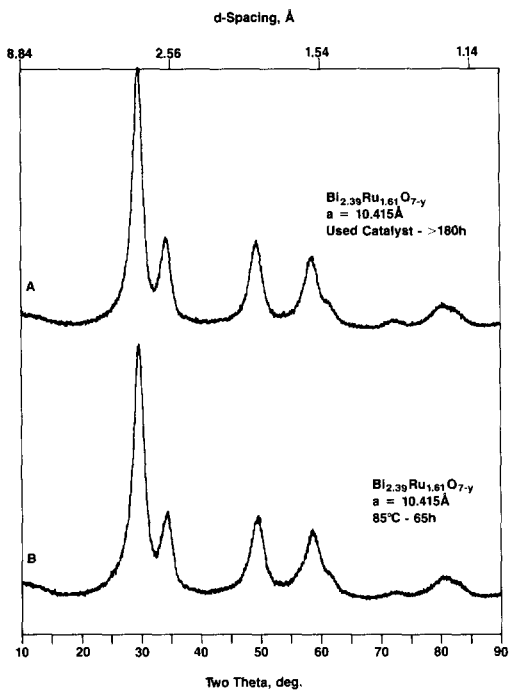

FIG. 5. Powder diffraction patterns for below 325-mesh powder of $Bi_{2.39}Ru_{1.61}O_{7-y}$ that was originally obtained as 40 to 60 mesh granules. The bottom tracing (B) shows the diffraction pattern obtained after the initial oxide synthesis. The top tracing (A) was obtained on the same sample that had been recovered after continuous oxidations for more than 180 hr with various substrates shown in Table 4.

the oxidations summarized in Table 4. Tracing B in Fig. 5 records the powder XRD pattern for an extra portion of the catalyst that was charged to the trickle bed reactor. The used granular catalyst was rinsed well in the reactor with water and then carefully recovered. After sieving the catalyst granules from the silica beads used for reactor packing, a total of 3.60 g of the dried catalyst was recovered, exactly the same amount as that originally charged. The recovered granules were ground to a fine powder and subjected to powder XRD analysis. Tracing A in Fig. 5 displays the powder XRD pattern for this used powdered catalyst. To within the accuracy of the XRD measurements, the poorly crystalline $Bi_{2.39}Ru_{1.61}O_{7-y}$ catalyst retained the same lattice constant and average crystallite size as when it was originally prepared. No change in the bulk structure is evident from these data. These results provide strong evidence for the chemical stability of the bismuth ruthenium pyrochlore oxides during the catalytic oxidation of substrates in aqueous alkaline solutions.

DISCUSSION

The results contained herein demonstrate that the same classes of organic substrates which were found to be electrochemically oxidized in aqueous alkaline solutions by expanded lattice ruthenium pyrochlore oxide anodes (*36–38*) are also oxidized by these same oxides directly with molecular oxygen at temperatures below 100°C without an externally applied potential. This can be perceived as a direct consequence of these electrically conducting materials to promote both anodic oxidation of organic substrates (*36–38*) and cathodic oxygen reduction (*62*). The initial motivation to examine heterogeneous mixed metal–ruthenium oxides came from the increasing number of studies reported with oxoruthenium complexes for the mediation of organic substrate oxidations (*77, 78*), even though these reported oxidations were chemically or electrochemically driven (*29, 35, 77–82*). Precedence for direct oxidations with molecular oxygen by certain oxoruthenium complexes has been established recently for some olefin epoxidations (*83–87*), alcohol-to-carbonyl group oxidations (*88, 89*), and oxidative dealkylation of tertiary amines (*90*). However, the use of a mixed metal oxide to perform liquid-phase oxidations with molecular oxygen at 25°C is reported here for the first time.

Evidence for Oxide Catalysis

In light of the unprecedented ability of the expanded lattice ruthenium pyrochlore oxides to catalyze oxidations with O_2 at temperatures below 100°C, it is relevant to inquire if the observed catalysis is in fact *cata-*

lytic and if it results from genuine heterogeneous catalysis. Evidence for *catalytic* operation of these $A_{2+x}Ru_{2-x}O_{7-y}$ compounds was presented in Tables 3 and 4. Substrate/catalyst ratios of above 1.0 and observation of oxygen uptake throughout the course of the oxidations suggest catalytic behavior by the oxides.

Three alternatives to genuine heterogeneous catalysis were cited by Ravno and Spiro (*91*) some 25 years ago: (1) reaction between the catalyst and the oxidant, (2) dissolution and reprecipitation of the catalyst, and (3) homogeneous catalysis by catalyst ions. Each of these alternatives must be considered as sources of catalytically active species. During the preparation of the expanded lattice ruthenium pyrochlore oxides in strongly alkaline solution ($[OH^-] > 3.0$), the effects described by (1) and (2) will occur to produce the final microcrystalline powders from soluble precursor ions. Effect (1) occurs when an oxidant, either in the form of an electrode with an externally applied potential (*92*) or molecular oxygen (*57*), reacts partially with the redox active surface ruthenium atoms to produce a soluble higher valent form of ruthenium (e.g., $Ru^{IV}O_2$ to $Ru^{VI}O_4^{2-}$) in alkaline solution (*93, 94*). The overall formation of the expanded lattice ruthenium pyrochlore oxide necessitates a dissolution-reprecipitation mechanism as described by effect (2) to convert the amorphous solid to the microcrystalline powder. Thus, in addition to the soluble ruthenium species during crystallization, formation of soluble forms of lead (*38*) and bismuth (*38, 95*) in alkaline solutions is necessary to produce higher valent forms of these ions in the $A_{2+x}Ru_{2-x}O_{7-y}$ compounds. A detailed treatment of the soluble species in equilibrium with the $A_{2+x}Ru_{2-x}O_{7-y}$ solid requires solubility product data on the various $A_{2+x}Ru_{2-x}O_{7-y}$ compounds as a function of temperature, $[OH^-]$, and applied potential (either from O_2 sparging or an anodic electrode (*92*)). This information is unavailable at this time.

Stable operation of the ruthenium pyrochlore catalysts for various organic substrates can be performed if the catalytic solid is used outside of the conditions in which the pyrochlore compound is crystallized. In the case of the $Pb_{2+x}Ru_{2-x}O_{6.5}$ compounds, soluble lead species are found even in weakly alkaline solutions (*38*). As seen in Table 1, a well-crystallized Pb–Ru pyrochlore compound with the formula $Pb_{2.06}Ru_{1.94}O_{6.5}$ is obtained from less than 1 *N* KOH solution without any O_2 sparging. Data of this type suggest that the poorly crystalline Bi–Ru pyrochlore compounds are better candidates for long-term catalyst stability testing. A test was conducted in a trickle bed reactor with catalyst granules having the bulk composition $Bi_{2.39}Ru_{1.61}O_{7-y}$. This catalyst was successful in selective catalytic oxidation of various 1,2-diols and primary alcohols for at least 180 hr at 55–95°C, 689 kPa O_2 pressure, and $[OH^-] < 2$. As noted in the Results section, no detectable amounts of either bismuth or ruthenium ions were found. Furthermore, the catalyst granules were recovered unchanged after operation with no measurable change in either the mass, crystallinity, or the bulk composition as determined by powder XRD data. These observations argue strongly against the participation of any homogeneous catalytic species (alternative (3) of Ravno and Spiro) in the organic substrate oxidations reported here. Evidence for finite catalyst solubility in 3 *N* KOH electrolyte solutions at 75°C was found when $A_{2+x}Ru_{2-x}O_{7-y}$ compounds were used as Teflon-bonded electrodes for oxygen reduction and evolution (*62*). Oxygen electrocatalysis data show the generation of small concentrations (1×10^{-5} *M*) of soluble *A* (*A* = Pb, Bi) and Ru species was dependent on $[OH^-]$, temperature, and the pyrochlore surface area. However, the observed electrocatalysis (*36–38, 62*) was attributed to the solid pyrochlore surfaces and *not* the solution soluble species. Control of $[OH^-]$ and the "reducing" environment provided by oxidizable organic

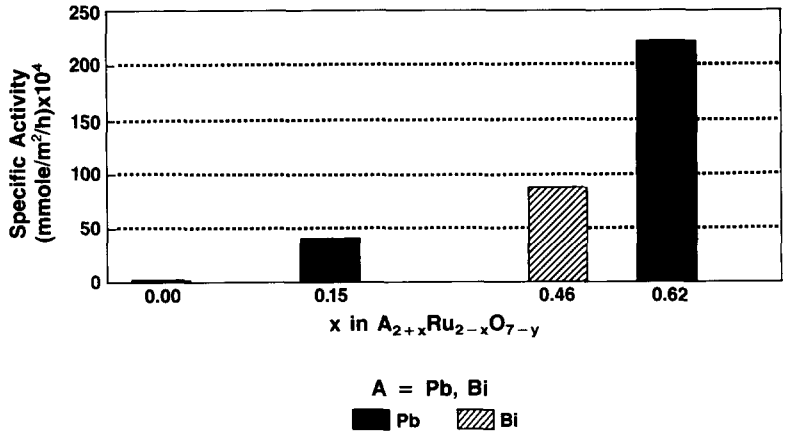

FIG. 6. Effect of the value of the lattice expansion parameter x on the specific activity of the powdered catalyst for the oxidative cleavage of *trans*-1,2-cyclohexanediol at 25°C in aqueous 1.5 *N* NaOH solution. The catalyst with $x = 0.0$ (Pb) shows no activity for selective conversion to adipate. The Bi-containing catalyst ($x = 0.46$) requires a temperature of 40°C before a comparable level of activity is found to that of the two Pb samples ($x = 0.15, 0.62$) shown here.

substrates ensure that at least some of the soluble species produced during the crystallization process (i.e., RuO_4^{2-}) will not be generated. On the basis of the effluent analyses during continuous trickle bed reactor operation, the reported liquid-phase oxidations described here are examples of *genuine heterogeneous catalysis*.

Activity Trends in Catalyst Composition and Substrate Type

Examination of the batch reactor data reveals several trends in catalytic oxidation activity of the expanded lattice ruthenium pyrochlore oxides. For a single substrate, *trans*-1,2-cyclohexanediol, the oxidative cleavage of TCD depends critically on the value of x in the general formula $A_{2+x}Ru_{2-x}O_{7-y}$. Figure 6 displays a bar graph of the specific activity defined by Eq. (4) for the $A_{2+x}Ru_{2-x}O_{7-y}$ catalysts plotted against the degree of substitution x by the post-transition metal atom. In general, an increase in the substitution of the post-transition metal atom in the ruthenium B-sites produces a more active catalyst toward the TCD substrate in aqueous alkaline solution. Three points emerge from the Fig. 6 bar graph: (1) the $Pb_{2.00}Ru_{2.00}O_{6.5}$ catalyst prepared by conventional ceramic methods is essentially inactive toward the oxidative cleavage of TCD; (2) the $Pb_{2.62}Ru_{1.38}O_{6.5}$ catalyst is some four to five times more active than the $Pb_{2.15}Ru_{1.85}O_{6.5}$ catalyst despite the fact that the latter catalyst has nearly twice the BET surface area as the former; and (3) the $Bi_{2.46}Ru_{1.54}O_{7-y}$ catalyst with almost four times the BET surface area as that of the $Pb_{2.62}Ru_{1.38}O_{6.5}$ catalyst requires a temperature of 40°C, but then it has activity comparable to that of the expanded lattice lead analogs at 25°C. This temperature variation suggests that there are slight electronic catalyst-substrate effects between the lead- and bismuth-expanded lattice ruthenium pyrochlore compounds that influence the catalytic activity toward TCD in addition to merely the available surface area. Differences in the oxide surface composition between these lead and bismuth ruthenium oxides are examined in the following paper (*66*).

The catalytic activity of the expanded lattice pyrochlore catalysts is also sensitive to the type of substrate. Figure 7 depicts a bar

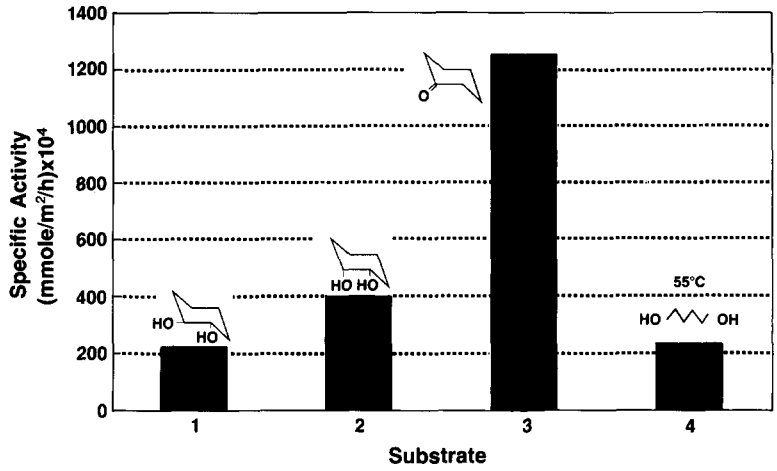

FIG. 7. Effect of the substrate on the specific activity of the $Pb_{2.62}Ru_{1.38}O_{6.5}$ catalyst to yield adipate product. Substrates 1–3 are catalytically oxidized at 25°C while substrate 4 requires a temperature of 55°C to produce a comparable level of activity. All oxidations are conducted in aqueous NaOH solution under 689 kPa O_2 pressure.

graph plot of the specific activity for the same $Pb_{2.62}Ru_{1.38}O_{6.5}$ catalyst toward four different C_6 oxygenate substrates. All substrates yield a common adipate product after catalytic oxidation in aqueous alkaline solution. The cyclohexanone substrate produces by far the highest catalytic activity. *Cis*-1,2-cyclohexanediol gives the next highest activity, a value that is about twice that of the *trans* analogue. Lastly, the 1,6-hexanediol substrate requires a temperature of 55°C in order to achieve comparable activity to that of TCD at 25°C. This order of functional group reactivity (ketone > 1,2-diol > primary alcohol) follows the same sequence as that when these $A_{2+x}Ru_{2-x}O_{7-y}$ oxides are used as anodic electrocatalysts (*36–38*). Qualitative trickle bed reactor data for oxidative cleavage of maleic acid and 2-butanol to 2-butanone oxidation indicate that these catalytic oxidations with molecular oxygen are much less efficient than those with ketone, 1,2-diol, or primary alcohol substrates. The electrocatalytic activity of various $A_{2+x}Ru_{2-x}O_{7-y}$ oxides for olefin oxidations has also been found to be low (*65*). These authors attributed the observed electrocatalytic activity toward olefinic substrates to the presence of a surface Ru(VI) species that forms with high surface areas for the bulk oxide.

Oxidized Substrates and Reaction Pathways

Oxidations proceed through reaction pathways mediated by either reagents or catalytic species that depend remarkably on the temperature and pH of the reaction medium (*96*). Comparative batch reactor data in Fig. 7 show that cyclohexanone is oxidized with the highest specific activity by the $Pb_{2.62}Ru_{1.38}O_{6.5}$ catalyst in aqueous alkaline solution. Oxidative cleavage of ketones is known to occur under both acidic (*97–99*) and basic (*100–103*) conditions and several cases give dicarboxylate products as found here directly with molecular oxygen (*97–99, 102, 103*). Regardless of the pH of the reaction medium, it appears that the reactive species for ketone substrates is the enol tautomer (*97, 100*). However, very recent kinetic studies at high temperatures and pressures in aqueous solutions suggest oxidation rates for cyclohexanone by homogeneous metal ions exceed the rate of enolization (*104*). As seen below, coordination of the

enolate form of cyclohexanone to the $Pb_{2.62}Ru_{1.38}O_{6.5}$ surface is consistent with the means by which 1,2-diol and primary alcohol substrates react. However, because ketones may oxidize through a number of possible pathways to yield dicarboxylate products (*97–103*), the $Pb_{2.62}Ru_{1.38}O_{6.5}$-catalyzed oxidation is not specific to ketone substrates.

In contrast to the molecular oxygen-driven oxidative cleavage of ketones by a number of catalysts, the selective oxidative cleavage of 1,2-diols with dioxygen to give dicarboxylate products appears specific to $A_{2+x}Ru_{2-x}O_{7-y}$ catalysts with perhaps only powdered silver-containing catalysts (*51*) as an alternative for this six-electron multistep oxidation. The need for alkaline reaction conditions prior to observation of any oxidation of the 1,2-diol substrate combined with the low ionization potential of diol oxygen lone pairs (*33*) suggest formation of a coordinated diol intermediate. While it can be stated with some certainty that the redox-active surface B-sites are likely points for this coordinated diol intermediate, a distinction between a high-valent post-transition metal atom (i.e., Pb(IV) or Bi(V)) and ruthenium assuming this B-site role cannot be made. On the one hand, Pb(IV) (*5, 7–10*) and Bi(V) (*11–16*) compounds are among the more effective reagents for two-electron 1,2-diol oxidative cleavage to dialdehyde products. On the other hand, oxoruthenium(IV) complexes are now known (*105*) to give hydroxo- and alkoxo-ruthenium(III) species with the alkoxo-ligands derived from primary or secondary alcohols. Alkoxo-ruthenium(III) complexes are prone to β-hydrogen elimination (*106*) with the resulting decomposition products undergoing further catalytic oxidation onto the observed products. These reduced ruthenium complexes are unstable in O_2-containing alkaline solutions (*93, 107*).

Further evidence to implicate the formation of a chelated diol intermediate on the pyrochlore oxide surface comes from a comparison of the specific activities for the TCD and CCD substrates with the $Pb_{2.62}Ru_{1.38}O_{6.5}$ catalyst shown in Fig. 7. Here the six-electron catalytic oxidation of CCD by $Pb_{2.62}Ru_{1.38}O_{7-y}$ proceeds at almost twice the rate of the TCD substrate. Studies of two-electron oxidative cleavage of 1,2-cyclohexanediol isomers by Pb(IV) (*108*) and periodate (*109–111*) show that the *cis* isomer is oxidized some 30 times faster than the *trans*. These studies with stoichiometric oxidants propose formation of a chelated intermediate originally suggested by Criegee for Pb(IV) tetraacetate (*108*). The rate enhancement observed for CCD oxidation over that of the TCD species has been attributed to a faster rate of decomposition of the *cis* isomer transition state and not to any difference in the ability of one isomer over the other to form a chelated intermediate. Chem-X molecular graphics comparisons of the CCD and TCD substrates coordinated to a metal atom (which may be part of the $A_{2+x}Ru_{2-x}O_{7-y}$ surface) show the O···O separations in the *cis* (2.85 Å) and *trans* (2.81 Å) forms of 1,2-cyclohexanediol to be practically the same. However, the TCD substrate is seen to project the cyclohexane ring away from the coordinated metal atom whereas the CCD substrate causes the cyclohexane ring to project perpendicular to the TCD C_6 ring conformation. This perpendicular C_6 ring for the *cis* isomer produces unfavorable steric interactions with the metal atom (or extended surface).

The overall oxidative cleavage of 1,2-diol substrates to dicarboxylate products proceeds through at least two distinct sequential reactions. The first reaction consists of the two-electron carbon–carbon bond cleavage depicted in Eq. (1) followed by two rapid two-electron oxidations of the aldehyde intermediates. These aldehydes account for the numerous by-products observed when the substrate/catalyst ratio is as high as that for some of the batch autoclave oxidations. Monocarboxylate products containing 15-, 17-, and 18-carbon atoms detected by GC/MS analyses arise through bimolecular aldol condensations of

these reactive aldehyde intermediates. Carboxyl-containing species of less than six (or less than multiples of six) carbon atoms are produced by at least two possible pathways (*112*). In the first such pathway, catalyst attack at the olefinic linkage formed from enolization of the aldehyde intermediate results in a mixture of C_1 and lower carbon chain carboxylate products. A second route for aldehyde oxidation involves free-radical hydrogen abstraction by the catalyst or components in the reaction medium followed by thermally driven decarbonylation of the carbonyl radical, again producing a mixture of lower carbon number carboxylate compounds. Oxygen atom incorporation into the aldehyde intermediates (the selective product pathway) may occur through either direct oxo group transfer from a surface Ru=O species or perhaps more likely, peracid formation through a radical chain process with O_2 (*113*) followed by efficient disproportionation of the peracid species by the $A_{2+x}Ru_{2-x}O_{7-y}$ surface. Previous electrochemical studies (*62*) have shown that ruthenium pyrochlore oxide anodes rapidly decompose H_2O_2 to water and oxygen with no detectable levels of H_2O_2 present.

In addition to 1,2-diol substrates, primary alcohols are oxidized to carboxylate products in high efficiency over $A_{2+x}Ru_{2-x}O_{7-y}$ oxides. Comparative batch autoclave reactor data from Table 3 show that 1,6-hexanediol begins catalytic oxidation (at a measurable rate) at a slightly higher temperature (55°C) than TCD over $Pb_{2+x}Ru_{2-x}O_{6.5}$ oxides. Excellent selectivities to adipate product (85–91%) are seen when HD is used as a substrate in 1.5 *N* NaOH in a trickle bed reactor. The HD oxidations proceed in high conversions over the $Bi_{2.39}Ru_{1.61}O_{7-y}$ catalyst granules. Supported Pt (*75*) and Pd (*95*) catalysts are reported also to give carboxylate products from primary alcohol substrates under basic reaction conditions. However, these catalysts typically show product inhibition on the reaction rate at high substrate conversions (>90%) in addition to deactivation effects, sometimes in the first batch reaction cycle (*75*). These problems are not observed with the ruthenium pyrochlore oxide catalysts in the data presented in Tables 3 and 4. A catalytic reaction sequence involving initial coordination of the alcohol (perhaps as an alkoxide ligand) similar to that for the 1,2-diol substrates appears likely in this eight-electron oxidation.

Recently, homogeneous trinuclear ruthenium complexes represented by $Ru_3O(O_2CC_2H_5)_6(PPh_3)_3$ were reported to oxidize primary and secondary alcohols with O_2 as the primary oxidant to aldehydes and ketones, respectively (*88*). Comparison of the catalyst turnovers reported for the two-electron oxidation of isopropyl alcohol to acetone by $Ru_3O(O_2CC_2H_5)_6(PPh)_3$ at 65°C and 276 kPa O_2 to those found here for the heterogeneous oxidation of HD at 75°C and 690 kPa O_2 (Table 4, entry 9) shows an advantage by the homogeneous catalyst. The trinuclear Ru complex produces 904 moles of product per mole of catalyst in 24 hr compared to only 46 moles of product per mole of $Bi_{2.39}Ru_{1.61}O_{7-y}$ catalyst in 24 hr from trickle bed reactor data. However, the HD oxidation represents an eight-electron oxidation (four times the moles of O_2 are required compared to the homogeneous complex). Additionally, the homogeneous catalyst is deactivated by increasing the temperature (or the pH), while the $Bi_{2.39}Ru_{1.61}O_{7-y}$ catalyst shows no deactivation at 95°C. At this temperature the heterogeneous catalyst produces 120 moles of adipate per mole of catalyst over a 24-hr period. No attempt was made to determine if combinations of higher temperatures and substrate flow rate would produce higher catalyst productivity, but pressure drop limitations were observed at flows approaching 100 ml/hr over the catalyst bed sizes used in Table 4.

The two-electron oxidation of 2-butanol to 2-butanone in aqueous buffered (pH 9.35) solution was examined in a trickle bed reactor over a $Bi_{2.86}Ru_{1.14}O_{7-y}$ catalyst. Qualitative ^{13}C NMR spectral analyses of the effluent solutions revealed 2-butanone to be the

principal product with small amounts of acetate by-product also detected. The estimated PROD and specific activity values are an order of magnitude less than those for the 1,2-diol and primary alcohol substrates run in a trickle bed reactor at the same reaction temperature. Clearly, for this oxidative dehydrogenation, the homogeneous trinuclear ruthenium complexes (*88*) described above provide a more effective means to catalyze this two-electron oxidation with molecular oxygen.

Two possible causes can account for the slow rate of conversion of the 2-butanol substrate. The oxidation is conducted in buffered solution and this lower pH value may slow the rate of catalyst reoxidation by O_2. A second possibility for the slow rate of 2-butanol oxidative dehydrogenation is the lack of a sufficient number of high valence-state ruthenium sites on the surface. Recent observations (*114*) on ruthenium complexes as alcohol oxidants point out that some ruthenium(IV) complexes will oxidize stoichiometrically alcohol substrates while ligation changes make alcohol oxidation possible on other ruthenium complexes only when ruthenium(V) is present. The successful use of a perruthenate reagent (i.e., Ru(VII)) for secondary alcohol-to-ketone conversions (*115*) further implies that the $A_{2+x}Ru_{2-x}O_{7-y}$ catalysts may not be able to generate such a high valence state of ruthenium under the reaction conditions used here.

In this work the oxidative cleavage of olefinic bonds is only slowly catalyzed by the ruthenium pyrochlore oxides. Maleic acid is cleaved to oxalic acid under strongly basic reaction conditions, but like the secondary alcohol-to-ketone oxidation discussed above, the bismuth ruthenate catalyst shows relatively low activity with only modest selectivity to dicarboxylate products (Table 5). The calculated PROD and specific activity values are over an order of magnitude lower than those of the 1,2-diol and primary alcohol substrates. Comparison of rates of electrocatalytic oxidation of these same types of functional groups over $Pb_{2+x}Ru_{2-x}O_{6.5}$ anodes shows the same order-of-magnitude difference in reactivity between olefinic and hydroxylated substrates (*37, 38*). A recent electrocatalytic study of alkene oxidations over variously prepared $A_{2+x}Ru_{2-x}O_{7-y}$ catalysts (*65*) concluded that the electroactive species toward olefin oxidation was a surface Ru(VI) site. This Ru(VI) species was present in greatest quantities on high surface area $A_{2+x}Ru_{2-x}O_{7-y}$ compounds. The $Bi_{2.30}Ru_{1.70}O_{7-y}$ catalyst used for catalytic oxidation of maleic acid has a surface area of 141 m^2/g, a value among the highest of the $A_{2+x}Ru_{2-x}O_{7-y}$ oxides examined here. Thus, an active Ru(VI) site does not appear to be generated under the catalytic oxidation conditions described here.

Oxygen Activation

While oxygen activation by *metal* catalysts occurs by means of dissociative chemisorption (*116*), oxygen is activated for use by oxidizable substrates over *metal oxide* catalysts by a variety of different ways. Reviews on various metal oxide catalysts that function at high temperatures with gas phase substrates generally treat oxygen activation in a phenomenological fashion (*117–119*) such that adsorbed dioxygen is reduced by four electrons in a sequence of steps eventually to lattice oxygen, O^{2-}. One or more of the reduced forms of O_2 may be used toward substrate oxidations. Liquid-phase oxidations of organic substrates with molecular oxygen in the absence of metal-containing catalysts occur under reaction conditions much more severe than those encountered in this work: 160 to 250°C and perhaps 6900 to 13800 kPa total pressure (*120*). The $A_{2+x}Ru_{2-x}O_{7-y}$ oxides used in this work are capable of O_2 reduction under much milder conditions than either the gas phase metal oxide catalysts or the uncatalyzed direct liquid phase substrates oxidations with O_2.

Electrochemical studies on the $A_{2+x}Ru_{2-x}O_{7-y}$ compounds (*62, 63, 65*) have reported the ability of these oxides to reduce

O_2 to water at low temperatures and also oxidize organic substrates with an applied electrical potential (*36–38, 65*). This work has shown that it is possible to combine oxygen reduction and substrate oxidation half-reactions to generate a catalytic cycle using O_2 as the terminal oxidant. These electrochemical studies have proposed various mechanisms by which O_2 is reduced including both inner (*62*) and outer (*63*) sphere schemes at the surface ruthenium sites. The inner sphere mechanism (*62*) involves O_2 reduction at a single surface ruthenium site with cycling between formal valence states of Ru(II) and Ru(VI). The outer sphere mechanism (*63*) includes a stepwise O_2 reduction with formation of an $HO_2^{\cdot}$ radical species. Both mechanisms were criticized (*65*) in terms of implausible intermediates: Ru(II) in the inner sphere case and $HO_2^{\cdot}$ formation in the outer sphere scheme. Consequently, a third mechanism was suggested (*65*) that rejected involvement of lattice oxygen and proposed that the O_2 reduction was a "suprafacial phenomenon."

While the above dioxygen reduction mechanisms lack molecular-level details, some elaboration of the third scheme above can be made through the reported structure of $Pb_2Ru_2O_{6.5}$ from powder neutron diffraction data (*121*). Figure 8 depicts the coordination geometries of the lead (distorted hexagonal pyramidal) and ruthenium (octahedral) atoms using the Chem-X software package. As an alternative to the single atom reduction of O_2, efficient four-electron reduction of O_2 can occur if two reduced metal centers are positioned spatially and electronically (filled antibonding orbitals for O_2 donation) for simultaneous μ-1,2-O_2 binding (*122*). As seen in Fig. 8, the columns of ruthenium atoms connected through μ-oxo bridges make attractive sites for pairwise O_2 binding when present in reduced surface states. The closest Ru···Ru separation in the $Pb_2Ru_2O_{6.5}$ structure is 3.61 Å (*121*), a distance appropriate for μ-1,2-O_2 binding (*122*). Support for this pairwise interaction of reduced ruthenium surface sites with O_2 in the $A_{2+x}Ru_{2-x}O_{7-y}$ compounds comes from both molecular complex analogies and hydrogen–oxygen gas adsorption measurements. Cleavage of dioxygen by various reduced transition metals has recently been demonstrated to produce M=O species directly (*123*). Dimeric ruthenium (III) alkyls have been shown to undergo oxidative addition with O_2 at -50°C to give dimeric ruthenium(V)–oxo alkyl complexes (*124*). An analogous reaction with O_2 is entirely possible on the reduced $A_{2+x}Ru_{2-x}O_{7-y}$ surface. Hydrogen chemisorptive titrations of several of the $A_{2+x}Ru_{2-x}O_{7-y}$ compounds reported in this work produce reduced surface (and surface-exposed bulk) ruthenium sites similar to the above ruthenium(III) alkyls (*124*). The reduced pyrochlore oxides react upon oxygen titration at various rates to reoxidize completely the reduced oxide. Details of these gas phase H_2–O_2 redox titrations along with additional analytical data on the $A_{2+x}Ru_{2-x}O_{7-y}$ oxides are presented in the following paper (*66*).

CONCLUSIONS

(1) Ruthenium pyrochlore oxides prepared by solution crystallization function directly with molecular oxygen for the catalytic oxidation of ketone; 1, 2-diol; primary alcohol; and olefin substrates to give carboxyl-containing products in aqueous alkaline solutions below 100°C. Retrospective analysis shows that these catalytic oxidations are expected from the dual electroactivity of these $A_{2+x}Ru_{2-x}O_{7-y}$ oxides for anodic organic substrate oxidations and cathodic O_2 reductions.

(2) For 1,2-diol substrates, expanded lattice ruthenium pyrochlores of the type $A_{2+x}Ru_{2-x}O_{7-y}$ with $A/Ru > 1.1$ are productive oxidative cleavage catalysts. Demonstrated product selectivities rival those of electrocatalytic methods.

(3) Functional group reactivity toward $A_{2+x}Ru_{2-x}O_{7-y}$ catalysts appears to follow

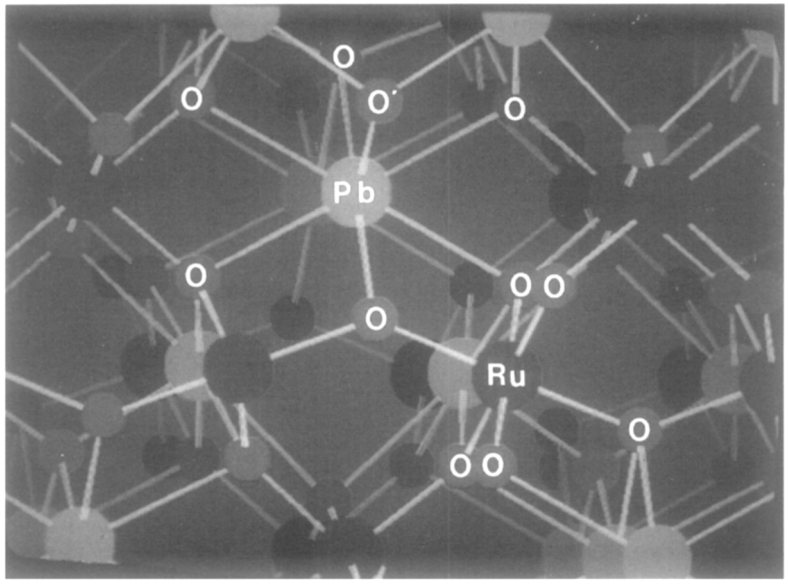

FIG. 8. View of the bulk coordination geometries found in $Pb_2Ru_2O_{6.5}$ showing a seven-coordinate Pb atom and a six-coordinate octahedral Ru atom. In the expanded lattice compounds, the higher valent lead atoms substitute into the octahedral Ru atom positions.

the same trends as those observed when these oxides function as anodic electrocatalysts: ketone > 1,2-diol > primary alcohol > olefin.

(4) Trickle bed reactor oxidations with $A_{2+x}Ru_{2-x}O_{7-y}$ catalysts afford higher product selectivities than the same oxidations conducted in batch autoclave reactors.

(5) Expanded lattice bismuth ruthenium pyrochlores, $Bi_{2+x}Ru_{2-x}O_{7-y}$, perform as stable heterogeneous catalysts under trickle bed reactor conditions with no detectable change in activity, mechanical integrity, or bulk composition ($x = 0.39$) after 180 hr of continuous operation.

ACKNOWLEDGMENTS

The authors gratefully acknowledge the contributions of the following individuals to this work: G. M. Wagner (technical assistance), J. R. Ebner (general discussions of oxidation catalysis), P. L. Mills (trickle bed reactors), D. E. Willis and J. T. Scanlon (analytical methods development), F. L. May (powder XRD data), B. R. Stults and M. R. Thompson (Chem-X modeling), J. J. Tria and S. K. Camden (BET surface area–pore volume data), and R. G. Kaley and R. C. Scheibel (GC/MS product analyses).

REFERENCES

1. Crutchfield, M. M., *J. Amer. Oil Chem. Soc.* **55,** 58 (1978).
2. Pfeifer, V. F., Sohns, V. E., Conway, H. F., Lancaster, E. B., Dabic, S., and Griffith, E. L., Jr., *Ind. Eng. Chem.* **52,** 201 (1960).
3. Stewart, R., "Oxidation Mechanisms, Applications to Organic Chemistry," pp. 97–106. Benjamin, New York, 1964.
4. Mehltretter, C. L., *in* "Methods in Carbohydrate Chemistry" (R. L. Whistler, Ed.), Vol. IV, pp. 316–317. Academic Press, New York, 1964.
5. Bunton, C. A., *in* "Oxidation in Organic Chemistry" (K. B. Wiberg, Ed.), Part A, pp. 367–407. Academic Press, New York, 1965.
6. Sklarz, B., *Quart. Rev.* **21,** 3 (1967).
7. Perlin, A. S., *in* "Oxidation, Techniques and Applications in Organic Synthesis" (R. L. Augustine, Ed.), Vol. 1, pp. 189–212. Dekker, New York, 1969.
8. Perlin, A. S., *in* "Carbohydrates, Chemistry and Biochemistry" (W. Pigman and D. Horton, Eds.), 2nd Ed., Vol. IB, pp. 1167–1215. Academic Press, New York, 1980.
9. Sheldon, R. A., and Kochi, J. K., "Metal-Cata-

lyzed Oxidations of Organic Compounds," pp. 143–144, 350–386. Academic Press, New York, 1981.
10. Rubottom, G. M., *in* "Oxidation in Organic Chemistry" (W. S. Trahanovsky, Ed.), Part D, pp. 1–145. Academic Press, New York, 1982.
11. Rigby, W., *Nature (London)* **164,** 185 (1949).
12. Rigby, W., *J. Chem. Soc.*, 1907 (1950).
13. Barton, D. H. R., Lester, D. J., Motherwell, W. B., and Barros Papoula, M. T., *J. Chem. Soc. Chem. Commun.*, 705 (1979).
14. Barton, D. H. R., Blazejewski, J.-C., Charpiot, B., and Motherwell, W. B., *J. Chem. Soc. Chem. Commun.*, 503 (1981).
15. Barton, D. H. R., Kitchin, J. P., Lester, D. J., Motherwell, W. B., and Barros Papoula, M. T., *Tetrahedron* **37** (Suppl. No. 1), 73 (1981).
16. Barton, D. H. R., Motherwell, W. B., and Stobie, A., *J. Chem. Soc. Chem. Commun.*, 1232 (1981).
17. Gut, G., Falkenstein, R. V., and Guyer, A., *Chimia* **19,** 581 (1965).
18. Kwart, H., Ford, J. A., Jr., and Corey, G. C., *J. Amer. Chem. Soc.* **84,** 1252 (1962).
19. Rocek, J., and Westheimer, F. H., *J. Amer. Chem. Soc.* **84,** 2241 (1962).
20. Epifanio, R. de A., Camargo, W., and Pinto, A. C., *Tetrahedron Lett.* **29,** 6403 (1988).
21. Konaka, R., and Kuruma, K., *J. Org. Chem.* **36,** 1703 (1971).
22. George, M. V., and Balachandran, K. S., *Chem. Rev.* **75,** 491 (1975).
23. Kaneda, K., Morimoto, K., and Imanaka, T., *Chem. Lett.*, 1295 (1988).
24. Kubias, J., *Coll. Czech. Chem. Commun.* **31,** 1666 (1966).
25. Richardson, W. H., *in* "Oxidation in Organic Chemistry" (K. B. Wiberg, Ed.), Part A, pp. 250–255. Academic Press, New York, 1965.
26. Freeman, F., *in* "Organic Syntheses by Oxidation with Metal Compounds" (W. J. Mijs and C. R. H. I. De Jonge, Eds.), Chaps. 2 and 5. Plenum, New York, 1986; Fetizon, M., Golfier, M., Mourgues, P., and Louis, J.-M., Chap. 10; Ho, T.-L., Chap. 11; Mihailovic, M. L., Cekovic, Z., and Lorenc, L., Chap. 14; Kitchin, J. P., Chap. 15; Ogata, Y., and Sawaki, Y., Chap. 16.
27. Zviely, M., Goldman, A., Kirson, I., and Glotter, E., *J. Chem. Soc. Perkin Trans. 1* 229 (1986).
28. Sugimoto, H., Spencer, L., and Sawyer, D. T., *Proc. Natl. Acad. Sci. USA* **84,** 1731 (1987).
29. Wolfe, S., Hasan, S. K., and Campbell, J. R., *J. Chem. Soc. Chem. Commun.*, 1420 (1970).
30. Greenspan, F. P., and Woodburn, H. M., *J. Amer. Chem. Soc.* **76,** 6345 (1954).
31. Huyser, E. S., and Rose, L. G., *J. Org. Chem.* **37,** 851 (1972).
32. Venturello, C., and Ricci, M., *J. Org. Chem.* **51,** 1599 (1986).
33. Shono, T., Matsumura, Y., Hashimoto, T., Hibino, K., Hamaguchi, H., and Aoki, T., *J. Amer. Chem. Soc.* **97,** 2546 (1975).
34. Ruholl, H., and Schaefer, H. J., *Synthesis*, 54 (1988).
35. Torii, S., Inokuchi, T., and Sugiura, T., *J. Org. Chem.* **51,** 155 (1986).
36. Horowitz, H. H., Horowitz, H. S., and Longo, J. M., *in* "Electrocatalysis" (W. E. O'Grady, P. N. Ross, Jr., and F. G. Will, Eds.), pp. 285–290. The Electrochemical Society, Pennington, NJ, 1981.
37. Horowitz, H. H., Horowitz, H. S., and Longo, J. M., US Patent 4,434,031 (1984).
38. Horowitz, H. S., Longo, J. M., Horowitz, H. H., and Lewandowski, J. T., *ACS Symp. Ser.* **279,** 143 (1985).
39. Hamilton, G. A., Reddy, C. C., Swan, J. S., Moskala, R. L., Mulliez, E., and Naber, N., *in* "Oxygenases and Oxygen Metabolism" (M. Nozaki, S. Yamamoto, Y. Ishimura, M.J. Coon, L. Einster, and R. W. Estabrook, Eds.), pp. 111–123. Academic Press, New York, 1982.
40. Ortiz de Montellano, P. R., *in* "Cytochrome P-450: Structure, Mechanism, and Biochemistry" (P. R. Ortiz de Montellano, Ed.), Chap. 7. Plenum, New York, 1986. Waterman, M., John, M. E., and Simpson, E. R., Chap. 10; Jefcoate, C. R., Chap. 11.
41. Murray, R. I., and Sligar, S. G., *J. Amer. Chem. Soc.* **107,** 2186 (1985).
42. Yuan, L.-C., Calderwood, T. S., and Bruice, T. C., *J. Amer. Chem. Soc.* **107,** 8273 (1985).
43. Okamoto, T., Sasaki, K., and Oka, S., *J. Amer. Chem. Soc.* **110,** 1187 (1988).
44. De Vries, G., and Schors, A., *Tetrahedron Lett.*, 5689 (1968).
45. Zeidler, U., Dohr, M., Lepper, H., Ger. Offen. 2,027,924 (1970) through *Chem. Abstr.* **76,** 45736e (1972).
46. Schrever, G., Schwarze, W., and Weigent, W., Ger. Offen. 2,052,815 (1972) through *Chem. Abstr.* **77,** 33963j (1972).
47. Camerman, P., and Hanotier, J., Fr. 2,095,160 (1972) through *Chem. Abstr.* **77** 125991v (1972).
48. Zeidler, U., Ger. Offen. 2,144,117 (1973) through *Chem. Abstr.* **78,** 135664a (1973).
49. Zeidler, U., and Lepper, H., Ger Offen. 2,256,888 (1974) through *Chem. Abstr.* **81,** 37251f (1974).
50. Zeidler, U., Ger. Offen. 2,314,454 (1974) through *Chem. Abstr.* **82,** 3811u (1974).
51. Lamberti, V., and Kogan, S. L., US Patent 3,873,614 (1975).
52. Rutledge, T. F., US Patent 3,860,642 (1975).
53. Nomiya, K., Miwa, M., and Sugaya, Y., *Polyhedron* **3,** 607 (1984).
54. Horowitz, H. S., Longo, J. M., and Haberman, J. I., US Patent 4,124,539 (1978).

55. Horowitz, H. S., Longo, J. M., and Lewandowski, J. T., US Patent 4,129,525 (1978).
56. Horowitz, H. S., Longo, J. M., and Lewandowski, J. T., *Mater. Res. Bull.* **16,** 489 (1981).
57. Horowitz, H. S., Longo, J. M., and Lewandowski, J. T., *Inorg. Synth.* **22,** 69 (1983).
58. Voorhoeve, R. J. H., Remeika, J. P., and Trimble, L. E., *Mater. Res. Bull.* **9,** 1393 (1974).
59. Goodenough, J. B., and Castellano, R. N., *J. Solid State Chem.* **44,** 108 (1982).
60. Carcia, P. F., Flippen, R. B., and Bierstedt, P. E., *J. Electrochem. Soc.* **127,** 596 (1980).
61. St. John, M. R., US Patent 4,395,316 (1983).
62. Horowitz, H. S., Longo, J. M., and Horowitz, H. H., *J. Electrochem. Soc.* **130,** 1851 (1983).
63. Egdell, R. G., Goodenough, J. B., Hamnett, A., and Naish, C. C. *J. Chem. Soc. Faraday Trans. I* **79,** 893 (1983).
64. Goodenough, J. B., Shukla, A. K., Silva Paliteiro, C. A. da, Jamieson, K. R., Hamnett, A., and Manoharan, R., PCT Int. Appl. WO 86/01642 (1986) through *Chem. Abstr.* **104,** 189805w (1986).
65. Van Veen, J. A. R., Van Der Eijk, J. M., De Ruiter, R., and Huizinga, S., *Electrochim. Acta* **33,** 51 (1988).
66. Felthouse, T. R., Fraundorf, P. B., Friedman, R. M., and Schosser, C. L., *J. Catal.* **127,** 421 (1991).
67. Felthouse, T. R., *J. Amer. Chem. Soc.* **109,** 7566 (1987).
68. Haymore, B. L., M. S. Thesis, Brigham Young University, 1972.
69. Van Rheenan, V., Cha, D. Y., and Hartley, W. M., *Org. Synth.* **58,** 43 (1978).
70. Felthouse, T. R., and Murphy, J. A., *J. Catal.* **98,** 411 (1986).
71. Germain, A., Crine, M., and Marchot, P., *in* "Chemical Engineering of Gas–Liquid–Solid Catalyzed Reactions" (G. A. L'Homme, Ed.), pp. 187–217. CEBEDOC, Liège, Belgium, 1979.
72. Ramachandran, P. A., Dudukovic, M. P., and Mills, P. L., *Sadhana* **10,** 269 (1987).
73. Willis, D. E., *Chromatographia* **5,** 42 (1972).
74. Hershman, A., unpublished observations.
75. Nicoletti, J. W., and Whitesides, G. M., *J. Phys. Chem.* **93,** 759 (1989).
76. Anderson, J. R., and Pratt, K. C., "Introduction to Characterization and Testing of Catalysts," Chap. 6. Academic Press, San Diego, CA, 1985.
77. Gore, E. S., *Plat. Met. Rev.* **28,** 111 (1984).
78. Sheldon, R. A., *Bull. Chem. Soc. Belg.* **94,** 651 (1985).
79. Moyer, B. A., Thompson, M. S., and Meyer, T. J., *J. Amer. Chem. Soc.* **102,** 2310 (1980).
80. Samuels, G. J., and Meyer, T. J., *J. Amer. Chem. Soc.* **103,** 307 (1981).
81. Thompson, M. S., De Giovani, W. F., Moyer, B. A., and Meyer, T. J., *J. Org. Chem.* **49,** 4972 (1984).
82. Meyer, T. J., *J. Electrochem. Soc.* **131,** 221C (1984).
83. Groves, J. T., and Quinn, R., *J. Amer. Chem. Soc.* **107,** 5790 (1985).
84. Groves, J. T., and Quinn, R., US Patent 4,822,899 (1989).
85. Taqui Khan, M. M., and Prakash Rao, A., *J. Mol. Catal.* **39,** 331 (1987).
86. Bailey, C. L., and Drago, R. S., *J. Chem. Soc. Chem. Commun.*, 179 (1987).
87. Leising, R. A., and Takeuchi, K. J., *Inorg. Chem.* **26,** 4391 (1987).
88. Bilgrien, C., Davis, S., and Drago, R. S., *J. Amer. Chem. Soc.* **109,** 3786 (1987).
89. Che, C.-M., Lai, T.-F., and Wong, K.-Y., *Inorg. Chem.* **26,** 2289 (1987).
90. Leising, R. A., Ohman, J. S., Acquaye, J. H., and Takeuchi, K. J., *J. Chem. Soc. Chem. Commun.*, 905 (1989).
91. Ravno, A. B., and Spiro, M., *J. Chem. Soc.*, 97 (1965).
92. Horowitz, H. S., Longo, J. M., and Lewandowski, J. T., *Mater. Sci. Monogr.* (React. Solids) **10,** 500 (1982).
93. Rard, J. A., *Chem. Rev.* **85,** 1 (1985).
94. Isherwood, D., "Application of the Ruthenium and Technetium Thermodynamic Data Bases Used in the EQ3/6 Geochemical Codes, UCRL-53594," NTIS Report DE85-013766 (1985).
95. Fiege, H., and Wedemeyer, K., US Patent 4,238,625 (1980).
96. Paderes, G. D., and Jorgensen, W. L., *J. Org. Chem.* **54,** 2058 (1989).
97. Den Hertog, H. J., Jr., and Kooyman, E. C., *J. Catal.* **6,** 357 (1966).
98. Roundhill, D. M., Dickson, M. K., Dixit, N. S., and Sudha-Dixit, B. P., *J. Amer. Chem. Soc.* **102,** 5538 (1980).
99. El Ali, B., Bregeault, J.-M., Mercier, J., Martin, J., Martin, C., and Convert, O., *J. Chem. Soc. Chem. Commun.*, 825 (1989).
100. Jones, D. D., and Johnson, D. C., *J. Org. Chem.* **32,** 1402 (1967).
101. Lissel, M., and Dehmlow, E. V., *Tetrahedron Lett.*, 3689 (1978).
102. Masilamani, D., and Manahan, E. H., US Patent 4,510,321 (1985).
103. Osowska-Pacewicka, K. and Alper, H., *J. Org. Chem.* **53,** 808 (1988).
104. Thomas, J. W., and Taylor, J. E., *Canad. J. Chem.* **67,** 165 (1989).
105. Nagao, H., Aoyagi, K., Yukawa, Y., Howell, F. S., Mukaida, M., and Kakihana, H., *Bull. Chem. Soc. Japan,* **60,** 3247 (1987).
106. Loren, S. D., Campion, B. K., Heyn, R. H., Tilley, T. D., Bursten, B. E., and Luth, K. W., *J. Amer. Chem. Soc.* **111,** 4712 (1989).

107. Rudd, D. P., and Taube, H., *Inorg. Chem.* **10,** 1543 (1971).
108. Criegee, R., Kraft, L., and Rank, B., *Justus Liebigs Ann. Chem.* **507,** 159 (1933).
109. Price, C. C., and Knell, M., *J. Amer. Chem. Soc.* **64,** 552 (1942).
110. Buist, G. J., Bunton, C. A., and Miles, J. H., *J. Chem. Soc.*, 743 (1959).
111. Honeyman, J., and Shaw, C. J. G., *J. Chem. Soc.*, 2454 (1959).
112. Riley, D. P., Getman, D. P., Beck, G. R., and Heintz, R. M., *J. Org. Chem.* **52,** 287 (1987).
113. McNesby, J. R., and Heller, C. A., Jr., *Chem. Rev.* **54,** 325 (1954).
114. Nugent, W. A., and Mayer, J. M., "Metal-Ligand Multiple Bonds," p. 270. Wiley, New York, 1988.
115. Griffith, W. P., Ley, S. V., Whitcombe, G. P., and White, A. D., *J. Chem. Soc. Chem. Commun.*, 1625 (1987).
116. Langmuir, I., *J. Amer. Chem. Soc.* **37,** 1139 (1915).
117. Bielanski, A., and Haber, J., *Catal. Rev. Sci. Eng.* **19,** 1 (1979).
118. Che, M., and Tench, A. J., *in* "Advances in Catalysis" (D. D. Eley, H. Pines, and P. B. Weisz, Eds.), Vol. 31, pp. 77–133. Academic Press, New York, 1982.
119. Centi, G., Trifiro, F., Ebner, J. R., and Franchetti, V. M., *Chem. Rev.* **88,** 55 (1988).
120. Taylor, J. E., and Weygandt, J. C., *Canad. J. Chem.* **52,** 1925 (1974).
121. Beyerlein, R. A., Horowitz, H. S., Longo, J. M., Leonowicz, M. E., Jorgensen, J. D., and Rotella, F. J., *J. Solid State Chem.* **51,** 253 (1984).
122. Collman, J. P., Anson, F. C., Bencosme, S., Chong, A., Collins, T., Denisevich, P., Evitt, E., Geiger, T., Ibers, J. A., Jameson, G., Konai, Y., Koval, C., Meier, K., Oakley, P., Pettman, R., Schmittou, E., and Sessler, J., *in* "Organic Synthesis Today and Tomorrow" (B. M. Trost and C. R. Hutchinson, Eds.), pp. 29–45. Pergamon, New York, 1981.
123. Cotton, F. A., and Wilkinson, G., "Advanced Inorganic Chemistry," 5th Ed., p. 451. Wiley, New York, 1988.
124. Tooze, R. P., Wilkinson, G., Motevalli, M., and Hursthouse, M. B., *J. Chem. Soc. Dalton Trans.*, 2711 (1986).